The Thesis Committee for Tyler Ian Davis
Certifies that this is the approved version of the following Thesis:

Design and Synthesis of Ligands for Luminescent Metal Complexes

APPROVED BY
SUPERVISING COMMITTEE:

Richard A. Jones, Supervisor

Emily Que

Design and Synthesis of Ligands for Luminescent Metal Complexes

by

Tyler Ian Davis

Thesis

Presented to the Faculty of the Graduate School of

The University of Texas at Austin

in Partial Fulfillment

of the Requirements

for the Degree of

Master of Arts

The University of Texas at Austin

August 2016

Acknowledgements

I'd like to thank my advisor, Dr. Richard Jones, for his kindness and support over the last few years. His example as an educator and authority figure is one that has influence how I will behave in similar roles in my future.

I'd like to thank all of my labmates, without whom I would have struggled to progress in my research. Their knowledge and willingness to help me is an inspiration. I would especially like to thank Matt Moore, for his extensive synthetic knowledge and recommendations for improving my synthetic strategies, Dan Strohecker, for his comradery and belief in my ability, and Kory Mueller, for his development of a new and exciting research project that I got to continue on with.

Thank you to my therapist, Kerry Miller, for helping me find myself and what I really want. I'm moving on with my life now, and I'm confident it'll only get better now.

Thank you to all of my friends for their support. Thank you for always listening to my problems and lifting me up when I was down. Thank you for giving me perspective and showing me what I couldn't see in myself. Thank you for relating to me and understanding what I was going through. Thank you so much Liam Taylor for giving me an outlet to have fun and socialize, and for reminding me of what I deserve for my efforts. A special thank you to Claudina Cammack, who always listened to me, encouraged me to continue on, and picked me up (sometimes literally) when I couldn't do it myself.

Finally, thank you to my mom and dad. I've gotten this far because of you. I don't always say it, but I love you both with all my heart. You've given me so much through my entire life. You taught me kindness and all I want is to pass that kindness on to everyone in my life.

Abstract

Design and Synthesis of Ligands for Luminescent Metal Complexes

Tyler Ian Davis

The University of Texas at Austin, 2019

Supervisor: Richard A. Jones

Luminescent metal complexes have been extensively investigated for a wide range of applications, including biological imaging and organic light emitting diodes (OLEDs). The ligand 2,6-bispyrazolepyridine (bppy) has shown itself to be an extremely effective sensitizer for Eu^{3+} complexes. Derivatives of this ligand have been synthesized with various oxygen containing groups attached at the 4 position of the pyrazoles. A novel diphosphine containing ligand with a terthiophene backbone has been synthesized. It is believed that this ligand could be used in Cu^{1+} complexes to create electropolymers capable of thermally activated delayed fluorescence (TADF).

Table of Contents

List of Figures

List of Schemes

CHAPTER 1: DEVELOPMENT OF LIGANDS FOR LUMINESCENT LANTHANIDE COMPLEXES

Introduction

LANTHANIDES

Lanthanides have found use in a wide range of applications including biological imaging,[1] catalysis,[2] NMR shift reagents,[3] chemical sensors,[4] thermometers,[5] magnets,[6] lasers,[7] luminescent thin films,[8] OLEDs,[9] and metallopolymers.[10] Many of these applications make use of the lanthanides' unique and interesting luminescent properties. Lanthanides exist primarily as Ln^{3+}, and the valence 4*f* orbitals are shielded by the filled 5*s* and 5*p* shells. This makes the lanthanides chemically very similar, and while this allows for ligand systems to be readily applied to most or all of the Ln^{3+} ions, it has also made separating them from one another very difficult.[11] In contrast to this, the lanthanides are electronically distinct. Because of the previously mentioned shielding of the 4*f* orbitals, the ligand environment of the Ln^{3+} metal center has a minimal effect on the electronic *f-f* transitions. This results in a line-like emission spectrum that is characteristic of the specific lanthanide. Free Ln^{3+} ions also have very small Stokes shifts for this same reason. Because these *f-f* transitions are Laporte- and spin-forbidden ($\Delta l = \pm 1$ and $\Delta S = 0$), the free Ln^{3+} ions typically have very low molar absorptivities and long excited state lifetimes in the milli- to microsecond range.

THE ANTENNA EFFECT

The poor absorptivity of the Ln^{3+} ions can be counteracted by indirect excitation. Strongly absorbing ligand chromophores are first excited which then transfer this energy to the lanthanide metal center, sensitizing them through a process known as the antenna effect (Fig 1.1). Energy transfer most commonly occurs from the antenna ligand excited triplet state to one of several excited states of the lanthanide.[12] For chromophores directly bound to a lanthanide metal center, this typically proceeds through a double electron transfer between energy donor and acceptor, known as a Dexter energy transfer (Fig. 1.2

a).[13] In the case of pendant chromophores that are attached through a separate binding site, Förster energy transference (Fig. 1.2 b) is responsible for lanthanide sensitization. In contrast to the Dexter mechanism that requires direct orbital overlap due to the electron exchange process, Förster energy transference occurs through space via long range dipole-dipole interactions up to 100 Å away.[13]

Deliberate selection and design of antenna ligands is required to improve the luminescence of these complexes. Common ligands for lanthanide complexes include substituted β-diketonates and derivatives of polyaromatic compounds such as naphthylene, tryphenylene and bipyridine.[14] Organic chromophores' good molar absorptivities, $\varepsilon \approx 10^4$-10^5 $M^{-1}cm^{-1}$ in the UV region, make up for the poor absorptivity of the Ln^{3+} centers, $\varepsilon \approx 1$-10 $M^{-1}cm^{-1}$.[13] Ligands predisposed to intersystem crossing to the excited triplet state are advantageous, as this is the primary position for energy transfer to the Ln^{3+} center to take place. Fortunately, spin-orbit coupling from the lanthanide improves intersystem crossing of the ligand S_1 to T_1 state.[15,16] For efficient energy transfer and to prevent thermal back energy transfer, the ligand excited triplet state should be at least 1850 cm^{-1} higher than the

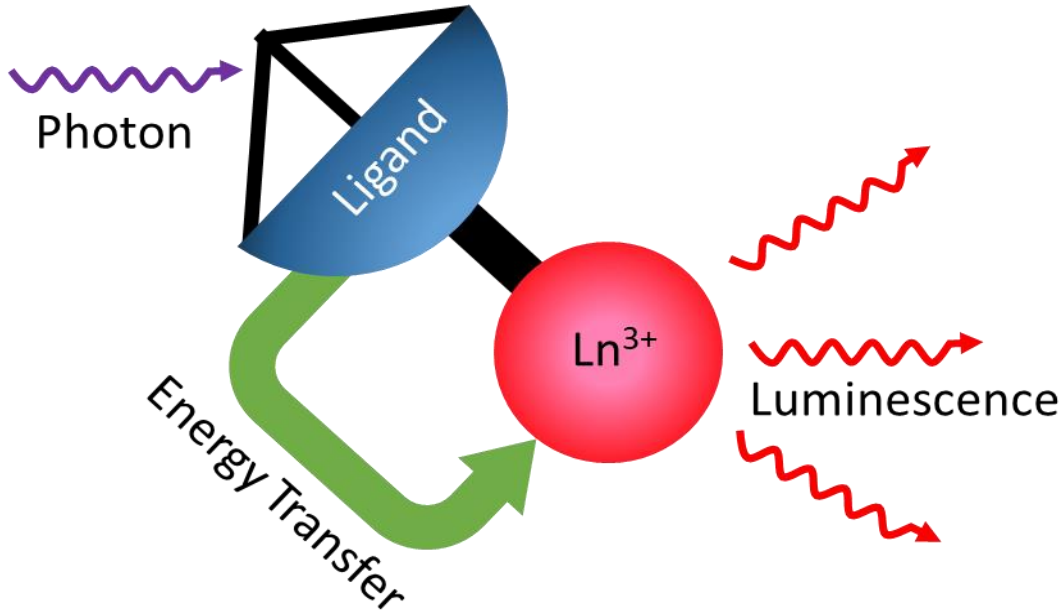

Figure 1.1: Diagram illustrating the antenna effect

Ln^{3+} excited state.[17] The quantum yield of lanthanide complexes is also maximized by reducing non-radiative pathways. Rigid ligand environments reduce these pathways. Fully coordinating the metal center also prevents water from binding directly, which significantly quenches the luminescence through O-H oscillations. [14, 18]

Although there are different methods in which to excite lanthanide metal centers[19,20] and the mechanisms by which they are sensitized by antenna ligands can be more complex,[1,21,14] the generally accepted simplified mechanism is laid out in Fig. 1.3. The antenna ligand is initially excited by an incident photon. The ligand then relaxes to its first excited singlet (S_1) state by internal conversion. The singlet state is generally considered too short lived to have a significant effect on the final excitation of the Ln^{3+} center. Energy not lost to fluorescence can then be transferred to the triplet state (T_1) by undergoing intersystem crossing. Energy not lost by phosphorescence at this point or non-radiative relaxation at any point in the process, can then be transferred from the ligand triplet state to the lanthanide excited state (Ln^{3+*}). Relaxation to the lanthanide ground state then results in the desired luminescence.

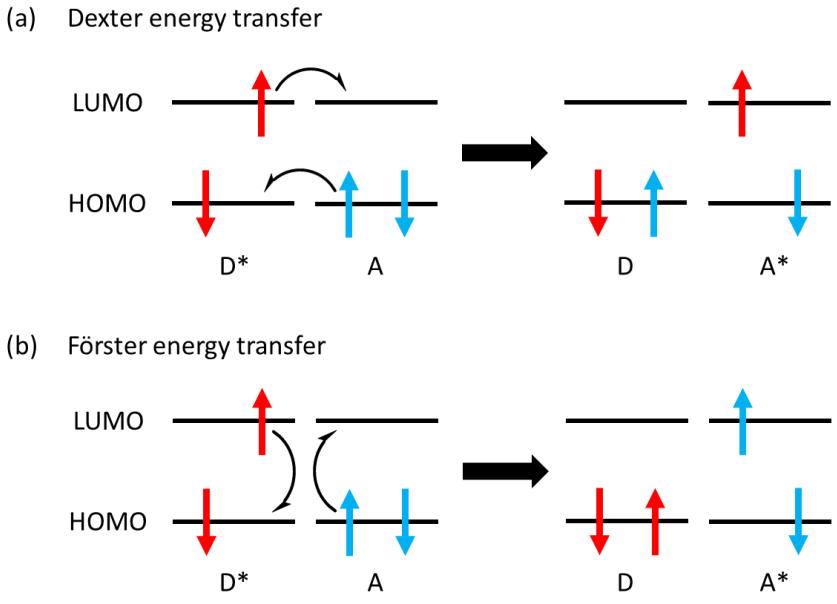

Figure 1.2: Illustration of a) Dexter and b) Forster energy transfer

BIOLOGICAL IMAGING

Several of the unique photophysical properties of lanthanides make them attractive for use in biological imaging.[1,14,22] In contrast to free Ln^{3+} ions which have minimal Stokes shifts, lanthanide complexes have very large pseudo Stokes shifts due to the down conversion of energy in the sensitization process. Many complexes have emissions in the NIR region, which allows for deeper tissue penetration. The long lifetimes of the *f-f* transitions make them suitable for time-resolved detection (TRD). This helps to maximize the signal to noise ratio that results from scattering and fluorescence of biological molecules. The narrow emission bands also allow for a narrow detection range to further limit noise.

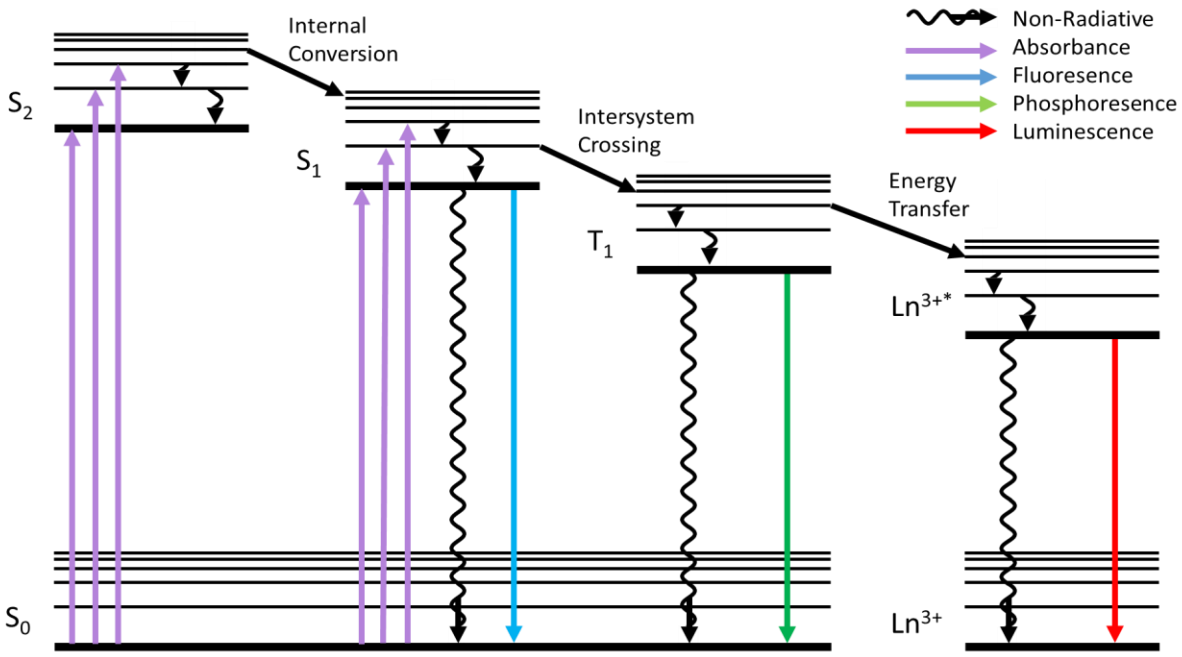

Figure 1.3: Jablonski diagram illustrating the energy transfer process from an antenna ligand to a lanthanide metal center

BPPY LIGAND SYSTEM

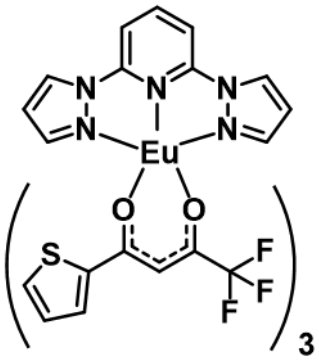

Figure 1.4: Europium(III) 2,6-bis(pyrazol-1-yl)pyridine tris(thenoyltrifluoroacetone) ($Eu(bppy)(tta)_3$)

Europium(III) tris(thenoyltrifluoroacetone) ($Eu(tta)_3$) (Fig. 1.4) is a very common parent complex for further functionalization, especially by addition of multidentate imine ligands (bipy, phen, terpy). It has been observed that the addition of 2,6-bis(pyrazol-1-yl)pyridine (bppy, **1**) results in the highest solid state quantum yield for a trivalent europium complex.[23] Several papers have been published that make use of functionalized Eu(bppy) complexes.[24-27]

Discussion

GOALS AND SCOPE OF PROJECT

The original goal was to make $Eu(bppy)(tta)_3$ soluble in water for eventual use in biological imaging applications. Further functionalization at the 4 position of the pyridine would then be used as a biological linker.[28] After significant setbacks, the scope of the project was changed to observe how varying oxygen containing electron withdrawing groups attached to the pyrazole (Pz) moieties would affect the luminescent properties of the corresponding Eu^{3+} complexes.

Scheme 1.1: Compounds Synthesized and Discussed in this Section

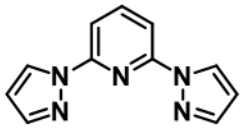

1
bppy

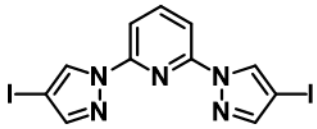

2
bppy-I

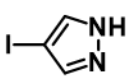

13
Pz-I

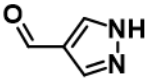

14
Pz-CHO

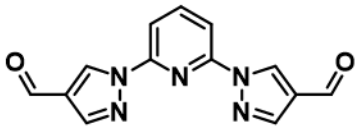

3
bppy-CHO

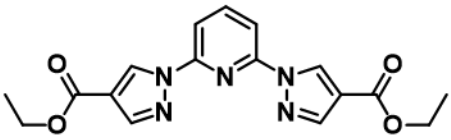

6
bppy-est

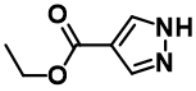

17
Pz-est

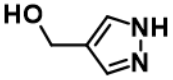

18
Pz-OH

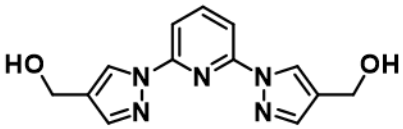

4
bppy-OH

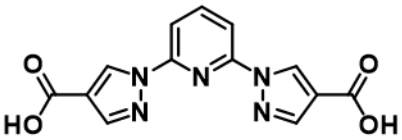

5
bppy-COOH

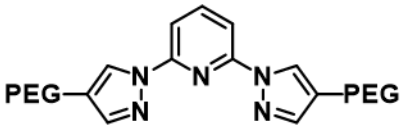

bppy-PEG

DIRECT BPPY FUNCTIONALIZATIONS

The relative ease of, albeit time consuming, synthesis of bppy[26] makes it an appealing starting point when considering how to further functionalize the molecule. The subsequent iodinization of the pyrazoles at the 4 position is also a very quick and easy process,[29] and both reactions can be done at gram scale. This functionalization opens up several options for aromatic substitution on the pyrazole rings. The free pyrazole groups can also be functionalized similarly before attachment to the central pyridine ring.[30]

The initially proposed synthetic route for a PEGilated bppy is illustrated in Scheme 1.2. Briefly, the parent bppy ligand was made and subsequently iodinized.[29] These iodines were then replaced in a Bouveault aldehyde synthesis.[29] The formyl groups were reduced to the alcohols by sodium borohydride. Separately, monomethoxytriethylene glycol

($CH_3(OCH_2CH_2)OH$) (PEG) was brominated (Br-PEG) in an Appel reaction.[31] Deprotonation of the pyrazole alcohols then allowed for a typical S_N2 reaction with the brominated PEG. This final product was chosen to provide a methylene spacer between bppy and the first oxygen atom, hopefully preventing any perturbation of the already desirable electronic energy levels of the parent bppy ligand. It was also hoped that providing this space would lessen the potential luminescent quenching from O···H vibrations between the PEG group and aqueous media.

Although this gave the desired product in overall 5 % yield, difficulties in replicating these reactions necessitated a search for alternative synthetic pathways for each of the intermediaries. The synthesis of the aldehydes was particularly frustrating. The original goal was eventually abandoned and the work repurposed to investigate how various oxygen containing groups attached to the pyrazoles affect the luminescent

Scheme 1.2: Initial Synthetic Route Towards a Water Soluble bppy

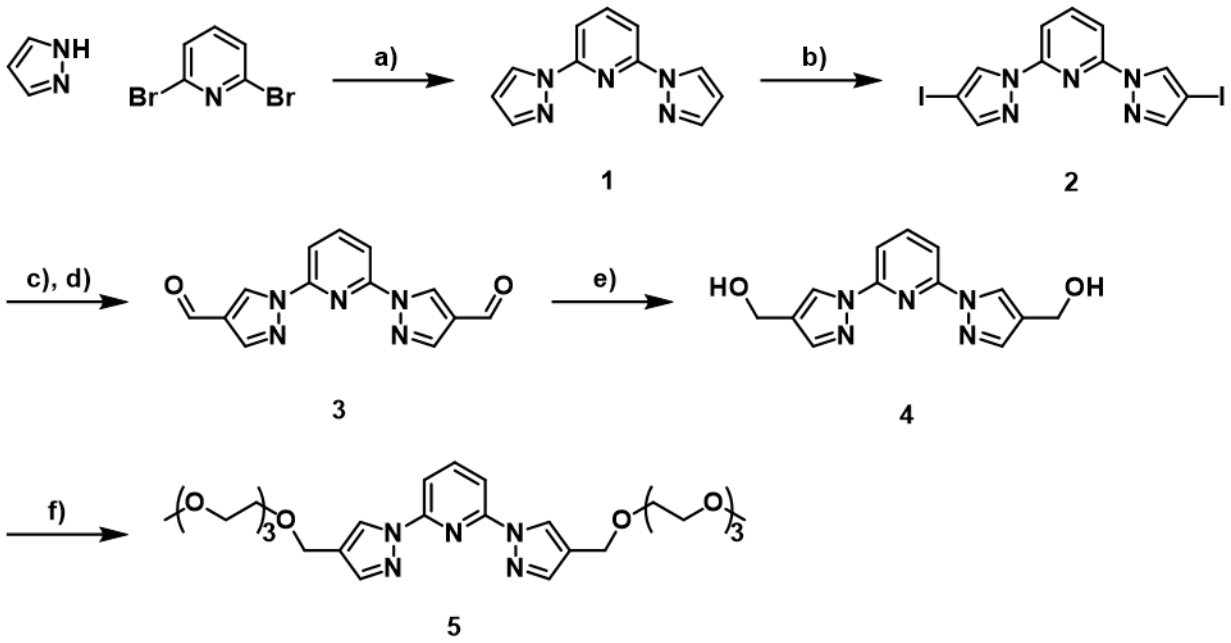

a) 2.5 NaH, diglyme, 120 °C, 5+ days b) 0.8 I_2, 0.2 HIO_3, AcOH, H_2O, H_2SO_4, 70 °C, 1 h. c) 2.2 *n*-BuLi, -78 °C, 2h d) 2.2 dimethylformamide, THF, 0 °C, 2h. e) $NaBH_4$, THF, 23 °C, 16 h. f) excess NaH, excess $CH_3(OCH_2CH_2)_3Br$, THF, 66 °C, 16 h.

properties of the final $Eu(tta)_3$ compounds. Although many of these compounds were synthesized, no metal complexes have been made with these ligands.

BPPY-CHO (3)

Scheme 1.3: Synthesis of Aldehyde Containing bppy

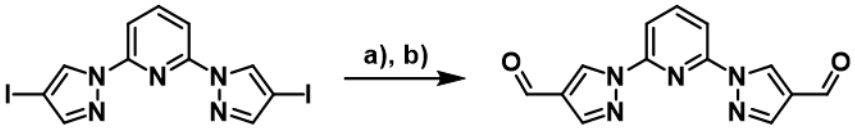

2 3

a) 2.2 *n*-BuLi, -78 °C, 2h b) 2.2 dimethylformamide, THF, 0 °C, 2h.

Formation of bppy-CHO was accomplished through a Bouveault aldehyde synthesis.[29] Most reactions either resulted in little-to-no yield of product or substances that appeared pure by NMR but had unreasonable yields of 200-400 % after using the published purification method. Separating the desired product from this apparently inorganic impurity was also exceptionally difficult as neither was appreciably soluble in common solvents besides DMSO, in which both dissolved. Using these crude products also resulted in very low yields for the subsequent reduction reactions. An attempt to directly make the Grignard from bppy-I (**2**) was similarly unsuccessful.

Because of the post-synthetic difficulties of this reaction, EtMgBr was substituted with *n*-BuLi as the sacrificial nucleophile. Indeed, the neutralization and purification were much simpler, but the desired result could not be replicated. In some instances, a significant portion of starting material was recovered.

BPPY-EST (6) AND BPPY-COOH (9)

Bppy-est was synthesized by the typical di-substitution of 2,6-dibromopyridine. This gave lower yields than the reaction of unsubstituted pyrazole moieties. This is likely because of the electron withdrawing nature of the ester group making the deprotonated

nitrogen of the pyrazolate a worse nucleophile. The asymmetric bppy-est$_1$ (**8**)was similarly made using the monosubstituted 2,6-di(pyrazol-1-yl)pyridine and Pz-est (**17**).

Although the previously established reaction is very consistent and relatively simple, the substitution proceeds very slowly and the reaction vessel is left at elevated

Scheme 1.4: Synthesis of Ester and Carboxylic Acid bppy Compounds

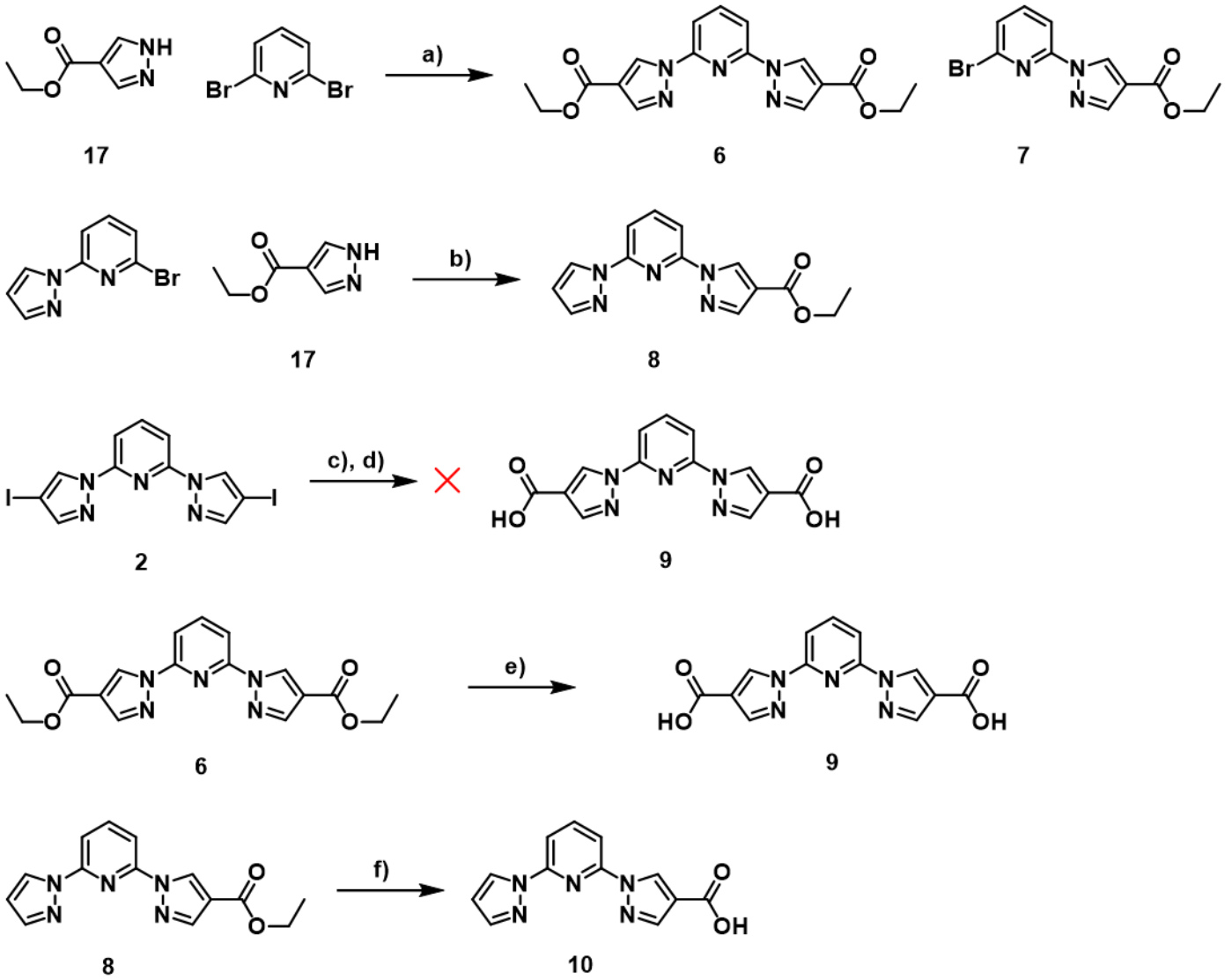

a) 2.5 NaH, diglyme, 120 °C, 7 days b) 1.3 NaH, diglyme, 120 °C, 3 days c) 2.2 *n*-BuLi, -78 °C, 2h d) excess CO_2(s), 23 °C, 16 h. e) 1.1 NaOH, 1:1 H_2O:EtOH, reflux, 1 h. f) 1.1 NaOH, 1:1 H_2O:EtOH, reflux, 3 h.

temperatures for up to a week. In an attempt to overcome these slow kinetics, the reaction was performed solvent free. This provides advantages in not requiring dry solvents, significantly decreased reaction time, and avoids the difficult process of removing diglyme from the process. The melting points of the reactants conveniently provide similar temperatures at which the standard reaction takes place. This reaction took place in less than one day and provided a similar yield for the disubstituted product, 43% for the conventional method vs. 31% for the neat reaction. This process has a lot of potential for optimization and can likely be applied to many other substituted varieties of pyrazole and pyridine.

Bppy-COOH was not successfully synthesized by reacting lithiated bppy-I and dry ice. Bppy-est was hydrolyzed to bppy-COOH in a basic ethanol and water mixture. This acid group could provide a handle for a variety of further functionalizations. The asymmetric bppy-$COOH_1$ (**10**) was also made in a similar fashion.

BPPY-OH (4)

$NaBH_4$ was used to reduce bppy-CHO. This reaction never produced the high yields (<20%) typically associated with these simple reductions. This is mainly attributed the starting bppy-CHO not being adequately made and purified, as stated previously.

Scheme 1.5: Synthesis of Alcohol bppy

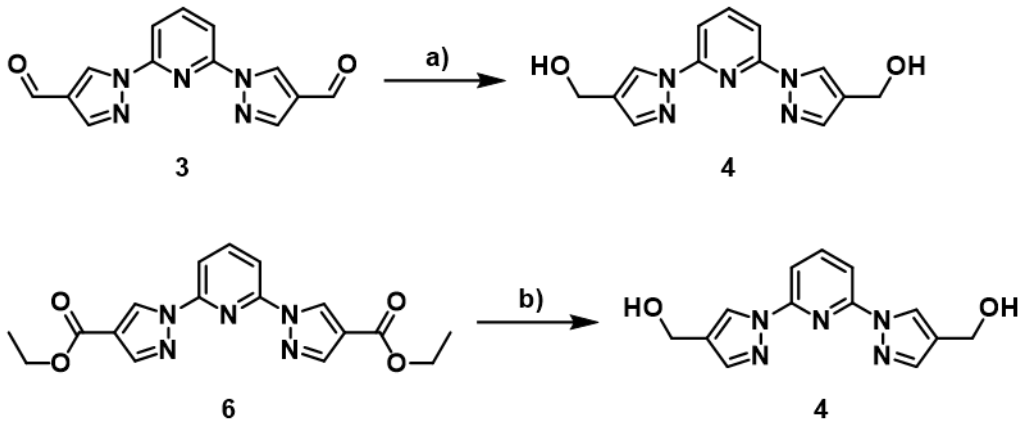

a) 1.5 $NaBH_4$, THF, 66 °C, 3.5 h. b) $LiAlH_4$, Et_2O, 23 °C, 3 h.

LAH was used in attempting to reduce bppy-est to the alcohol. Although the desired product was observed by mass spec and NMR, it was never successfully collected

BPPY-PEG

This section references any form of attachment of a triethyleneglycol group to the parent bppy molecule, regardless of starting materials and number of carbon spacers between bppy and the first O atom of the PEG chain.

The original target molecule (**5**) was made by reacting bppy-OH with significant excesses of both base and Br-PEG ($CH_3(OCH_2CH_2)_3Br$) (bppy-OH : NaH : Br-PEG was 1:18:47). This was done to try to maximize the yield of the desired product as there was only a minimal amount of bppy-OH available at the time. Further iterations of this reaction would likely have been carried out with more typical reactant ratios, but workable amounts

Scheme 1.6: Synthesis of PEGilated bppy Compounds

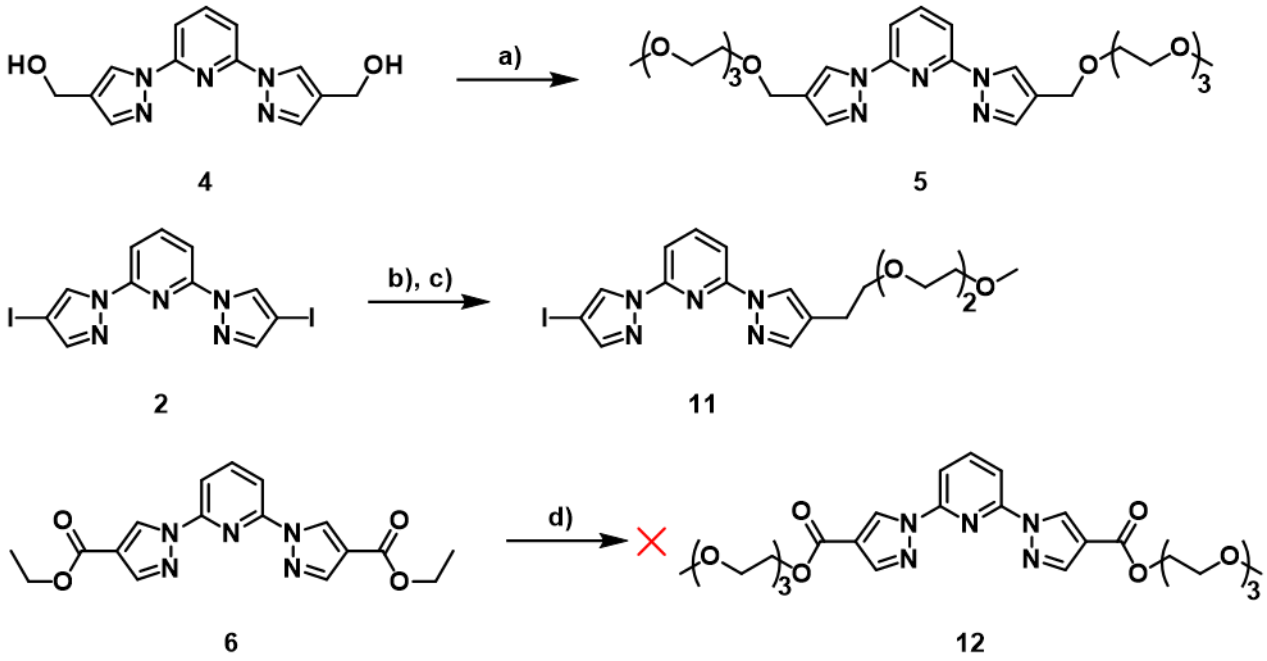

a) excess NaH, excess $CH_3(OCH_2CH_2)_3Br$, THF, 66 °C, 16 h. b) 4 *n*-BuLi, 1:1 THF:Et_2O, -78 °C, 2h. c) 5 $CH_3(OCH_2CH_2)_3Br$, 23 °C, 16 h. d) excess $CH_3(OCH_2CH_2)_3OH$, H_2SO_4, EtOH. reflux. 30 min.

of bppy-OH could not be synthesized again. Finding a method of purification for this product was very difficult, requiring two separate columns to isolate the product. After the first column, the major impurity was dimethoxyhaxaethylene glycol ($CH_3(OCH_2CH_2)_6OCH_3$) resulting from the reaction between Br-PEG and its hydrolyzed version (($CH_3(OCH_2CH_2)_3OH$).

Coupling Br-PEG to a lithiated bppy-I gave only a small yield (9%) of the monosubstituted product. This, in addition to the many failures in attempting to formylate bppy-I through lithiation, suggest that lithiations are unsuitable for bppy-I. It could be that the lithiated, and especially the di-lithiated, intermediaries are too electron rich to form or too unstable to survive the reaction.

A single attempt was made to form a PEGilated bppy by transesterification of bppy-est and monomethoxytriethylene glycol. Unfortunately this reaction failed, but likely only because the reaction was heated directly on a hot plate and not regulated by an oil bath, resulting in thermal decomposition of one or both reactants.

PYRAZOLE FUNCTIONALIZATION

Pz-CHO (**14**) was formed from Pz-I (**13**) in a Bouveault aldehyde synthesis, but unfortunately resulted in very small yield (15 %).[32] Additional equivalents of *n*-BuLi are required for this reaction to first deprotonate the pyrazole.[32] To adjust this need and to move to a less harsh sacrificial nucleophile, the pyrazole was protected by ethyl vinyl ether.[33,34] This protecting group should be stable to these conditions and easily removed. Unfortunately this reported process was not replicated.[33,34] A Vilsmeier–Haack reaction was also attempted on a similarly protected, unsubstituted pyrazole, but again did not provide the desired product.

Reduction of Pz-est to Pz-OH (**18**) by LAH is very straightforward. The reaction requires an additional equivalent of LAH to first deprotonate the pyrazole. Strangely, even when using excess LAH, this reaction only gave ~50% yield every time it was attempted. Typical ester reductions with LAH give nearly full conversion to the alcohol.[35] It could be

that the Pz needs to be protected before the reduction.[36] Reduction of a BOC protected Pz-est by $NaBH_4$ did not give the desired product.

ULLMANN COUPLING

Ullmann type coupling reactions have shown some promise in directly PEGilating bppy-I or Pz-I, but have run into synthetic complications or have resulted in unexpected products (Scheme 1.7). These types of reactions were originally made for coupling of aryl halides[37], but have found use to convert aryl halides to ethers, thioethers and amines.[38]

Scheme 1.7: Functionalization of Pyrazole Compounds

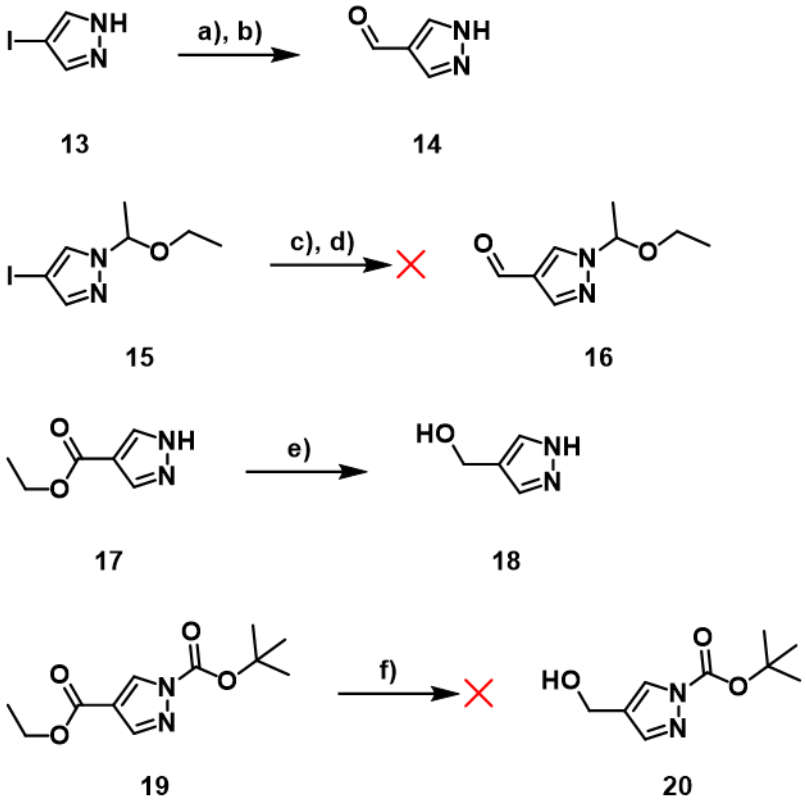

a) 3 *n*-BuLi, THF, -78 °C, 30 min., then 23 °C, 3.5 h. b) 1.2 dimethylformamide, -78 °C, 1 h., then 23 °C, 16 h. c) 2.5 EtMgBr, THF, 0°C, 1 h. d) 1 dimethylformamide, 23 °C, 30 min. e) 3 $LiAlH_4$, THF, 23 °C, 16 h. f) 3 $NaBH_4$, THF, 66 °C, 4 h.

It is very common for these catalysts to contain multidentate aromatic nitrogen donor ligands, such as bipyridine or phenanthroline, to improve catalytic efficiency and lower the reaction temperature.[38] For this reason, the reaction was first attempted with only CuI, bppy, PEG, and base, hoping that bppy would act as the supporting ligand for its own reaction. Unfortunately this was not the case, and no product was observed. Using

Scheme 1.8: Products of Ullmann Coupling Reactions

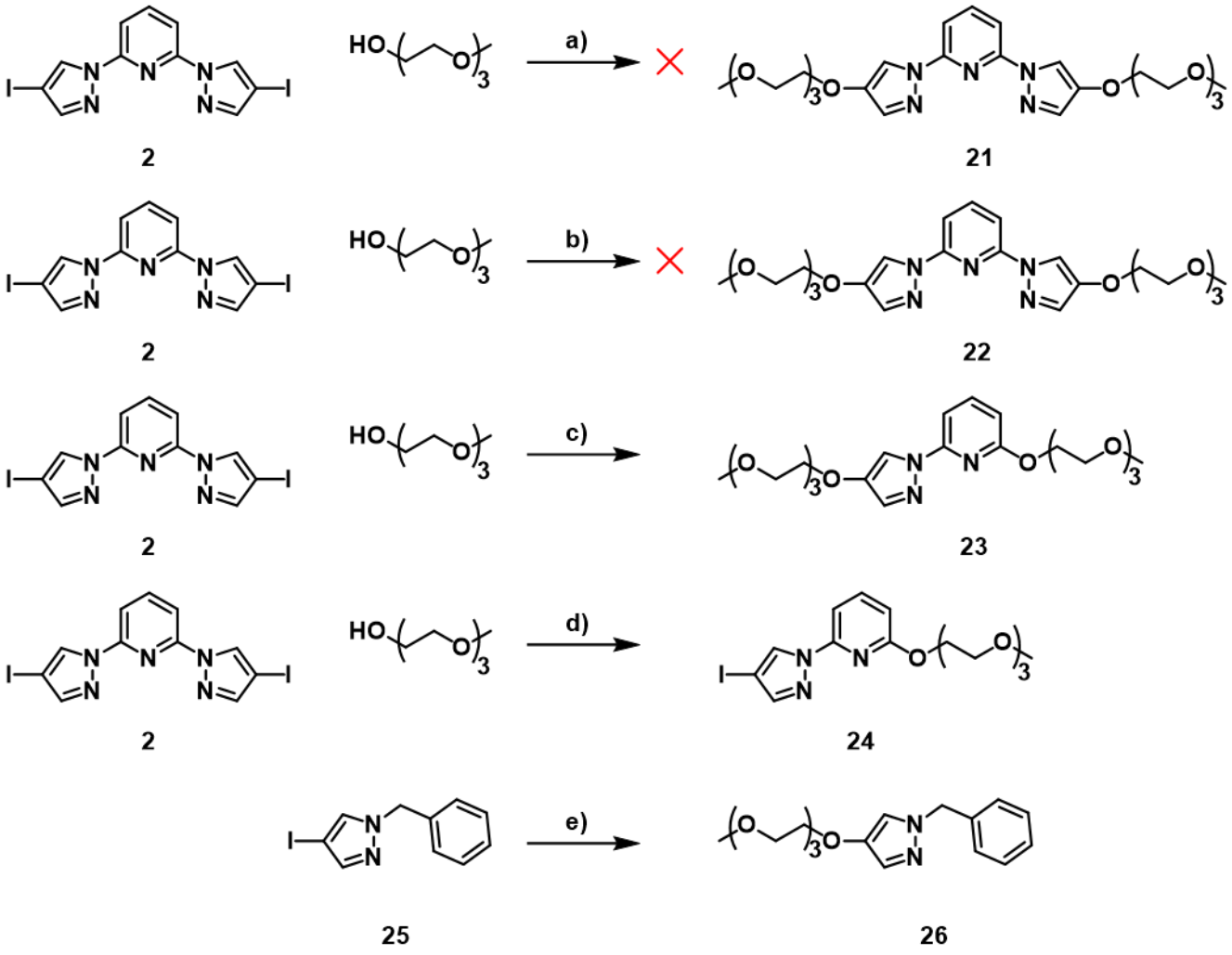

a) 4 Cs_2CO_3, 0.10 Cu_2O, THF, 66 °C, 16 h. b) 4 Cs_2CO_3, 0.12 CuI, dioxane, 101 °C, 16 h. c) 4 Cs_2CO_3, 0.10 [Cu(phen)]I, excess monomethoxytriethylene glycol, 122 °C, 20 h. d) 3 K_3PO_4, 0.05 $[Cu(bipy)_2]BF_4$, excess monomethoxytriethylene glycol, 122 °C, 20 h. e) excess $CH_3(OCH_2CH_2)_3OH$, 3 K_3PO_4, 0.1 CuI, 0.2 neocuproine, 115 °C, 2d.

phenanthroline as the catalyst ligand resulted in one successful coupling of PEG to one pyrazole, but resulted in the substitution of the other pyrazole, PEGilating the pyridine. This was actually the main product of the reaction, rather than an unwanted side product. Next, two equivalents of bipyridine as the catalyst ligands were used to create a slightly less reactive catalyst. Unfortunately, this resulted in a selective substitution of one pyrazole ring over the iodide as the major product. It's difficult to speculate a cause for this odd chemistry, but one explanation is that the bppy compound is binding differently than a typical aromatic would in the catalytic process because of the hetero atoms. It could also be competing with the catalytic ligands and affecting the reactivity negatively in this way.

For Pz-I, it seems to be necessary to protect the amine nitrogen of the ring. Reactions using excess base to deprotonate both the pyrazole and PEG chain did not work. Attempts with two separate bidentate catalytic ligands, phenanthroline and neocuproine, were likewise unsuccessful for unprotected Pz-I PEGilation. Pz-I protected with a benzyl group works with moderate yield, but the subsequent deprotection using H_2 and a Pd/C catalyst seems to destroy the molecule.

Conclusion

A large variety of synthetic pathways have been investigated towards functionalizing bppy with various oxygen containing functional groups. Reactions that involve strong nucleophiles, such as EtMgBr, *n*-BuLi, and LAH, can give the desired product to some extent but also result in unexpected and unwanted biproducts. In Ulmann-type coupling reactions, bppy also reacts in very unexpected ways. Similar reactions with Pz derivatives are more well behaved.

A new solvent-free method of pyrazole substitution onto 2,6-dibromopyridine was investigated. This method is significantly faster than refluxing in diglyme and does not need to deal with removing this solvent before purification. A similar product yield was obtained using this method and can still be further optimized.

CHAPTER 2: THERMALLY ACTIVATED DELAYED FLUORESCENCE OF COPPER COMPLEXES WITH NEW TERTHIOPHINE BISPHOSPHINE LIGAND

Introduction

ORGANIC LIGHT EMITTING DIODES

Organic light-emitting diodes (OLEDs) have been the subject of extensive research in recent years, in large part because of their extensive commercial applications in lighting and screen displays.[39-42] OLEDS can be made thinner and on more flexible substrates than typical LED or LCD displays. OLED displays also use less energy than LCD screens because they do not require a backlighting source. The fabrication process can also be less expensive and simplified.[43] This also makes them more suitable for large area displays.

OLEDs made from typical organic molecules emit by fluorescence (Fig. 2.1 a), but due to the nature of electroluminescence, electron-hole pairs (excitons) form in a statistical

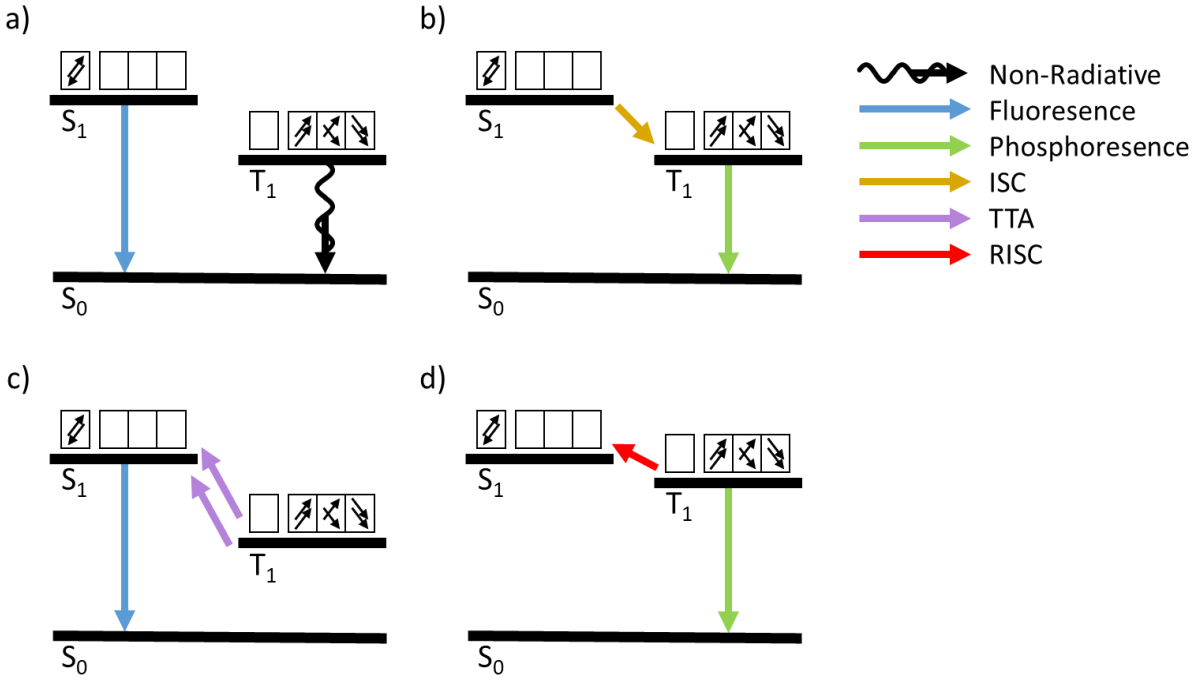

Figure 2.1: Illustrations of the various emission mechanisms used in OLEDS. a) fluorescence, b) phosphorescence, c) tritplet-triplet annihilation, and d) thermally activated delayed fluorescence

distribution of singlet and triplet states. This limits the device's internal quantum efficiency (IQE) to 25%.[39,44] Several different approaches can be taken to make use of the triplet excitons. Triplet-triplet annihilation (TTA), also known as triplet-triplet fluorescence (TTF), takes the energy of two triplet states and upconverts them to a singlet excited state which then fluoresces, resulting in a theoretical IQE of 62.5% (Fig. 2.1 c).[45,46] One of the most common methods of harvesting the triplet state is to use heavy metal complexes with high spin orbit coupling to relax the selection rules to promote intersystem crossing (ISC) and phosphorescence, resulting in a maximum IQE of 100% (Fig. 2.1 b).[47,48] Another way to make use of the triplet excitons is by adjusting the energy levels of the singlet and triplet states to be close enough in energy that the triplet electrons can thermally back populate the singlet state by reverse intersystem crossing (RISC), and thus emit by fluorescence. This process, known as thermally activated delayed fluorescence (TADF), also has a theoretical IQE of 100% (Fig. 2.1 d), and will be discussed in more detail in the following section. It should be noted that although the IQE of such devices may be quite high, device construction attenuates the external quantum efficiency (EQE) of any device.[49,50]

THERMALLY ACTIVATED DELAYED FLUORESCENCE

TADF occurs when the T_1 state populates the S_1 state where fluorescence can occur efficiently. To do this, the energy difference between the S_1 and T_1 (ΔE_{ST}) states must be minimized. This allows the thermal back-population from T_1 to S_1 by RISC. (Fig. 2.2). The temperature dependence of this process is related to the Boltzmann distribution:

$$k_{RISC} = k_{ISC} \cdot exp\left(-\frac{\Delta E_{ST}}{k_b T}\right) \qquad 2.1$$

Where k_b is the Boltzmann constant, T is temperature, and k_{RISC} and k_{ISC} are the rate constants for RISC and ISC, respectively.[51] From this equation, it is apparent that minimizing ΔE_{ST} increases the rate of RISC to be and therefore the effectiveness of the TADF process.

Minimizing ΔE_{ST} can be done by spatially separating the HOMO and LUMO. This can be done through bulky separated donor-acceptor hybrid molecules,[52-54] or orthogonally

directing the orbitals of the molecule such as in spiro compounds[55] or tetrahedral metal complexes.[56] Fullerenes also exhibit TADF,[57-59] and more novel methods of separating the HOMO and LUMO have also been studied.[60]

TADF emitters are attractive for OLED applications because they remove the need for expensive heavy metals, like Pt and Ir, to harvest triplet excitons by phosphorescence.[48] Ir and Pt complexes, such as platinum octaethylporphyrin (PtOEP) and tris[2-phenylpyridinato-C^2,N]iridium(III) ($Ir(ppy)_3$) (Fig. 2.3), have been used extensively for this reason.[61-63] Purely organic TADF emitters have been studied extensively.[64,65] Compounds have been synthesized that emit across the entire visible spectrum,[64,66]

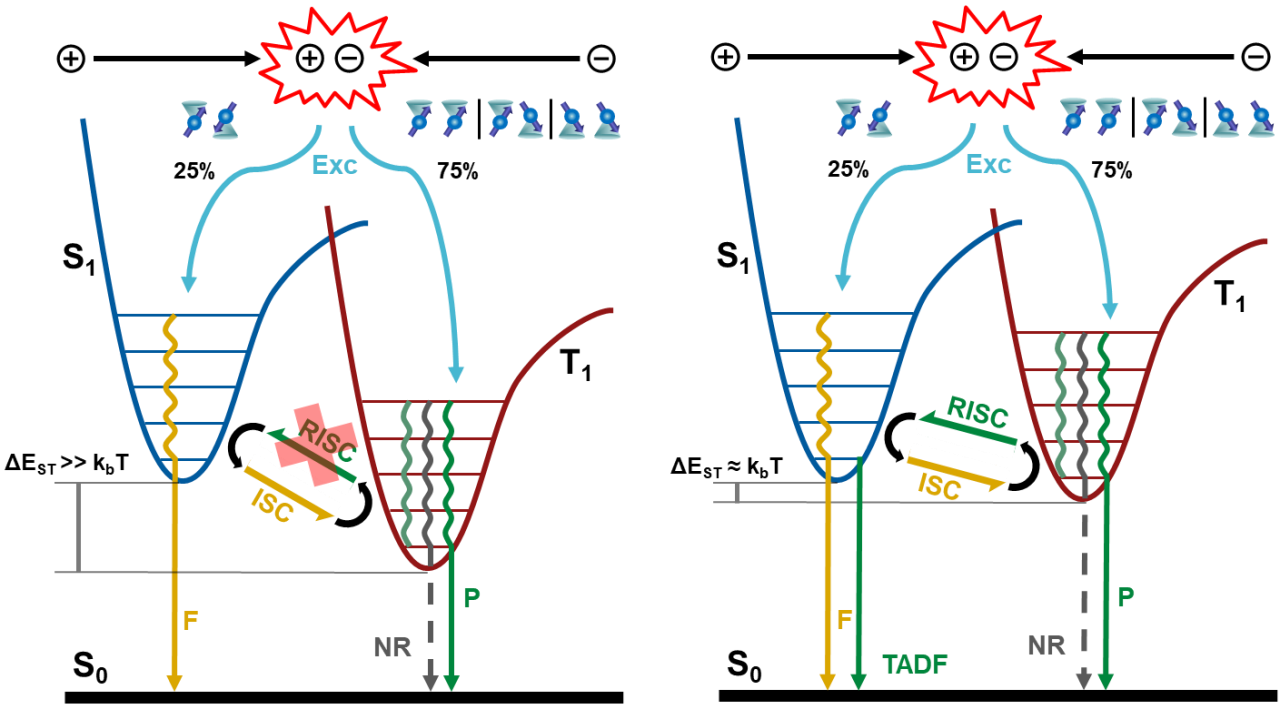

Figure 2.2: Illustration for the processes involved in the electroluminescence of OLEDS. Electron-hole recombination of the emissive material generates a statistical distribution of singlet and triplet excitons. a) Simple fluorescent OLEDs emit from the excited singlet state while the triplet state relaxes non-radiatively. Heavy metals with strong spin-orbit coupling can be used to promote ISC and phosphorescence to harvest all excitons. b) TADF emitters are designed to minimize the energy gap between the singlet and triplet excited state to allow efficient RISC to the singlet state where fluorescence can occur efficiently.

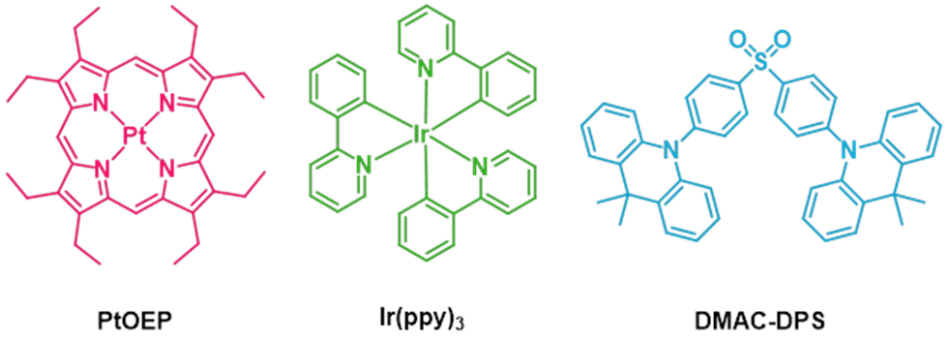

Figure 2.3: Examples of common compounds used in OLEDs

including blue light that phosphorescent materials often struggle with.[67] In fact, blue TADF emitters, such as diphenylsulfone dimehtyldihydroacridine (DMAC-DPS), have already seen use in OLEDs.[68]

TADF compounds also have several other applications. Because triplet excitons are sensitive to oxygen, the quenching of the delayed fluorescence can be used as an exceptionally sensitive oxygen sensor.[69] The temperature dependence of the TADF process also makes the suitable as sensitive thermometers.[70] Because the S_1 state of a molecule is populated by the T_1 state, they can exhibit fluorescence lifetimes that are more characteristic of phosphorescence, in the micro- to millisecond range.[71] This makes them suitable for time resolved biological imaging.[72] Photocatalytic systems involving TADF compounds have also been investigated for applications such as water splitting.[73]

COPPER FOR TADF

Copper(I) complexes have been studied extensively for their applications in TADF.[56,74] Because these complexes contain a d^{10} metal center, they prefer a tetrahedral geometry. This easily aligns two bidentate ligands orthogonally to one another. This feature can be exploited to separate the HOMO and LUMO of the complex and minimize ΔE_{ST}. Other common structures for Cu(I) TADF complexes include trigonal-planar compounds made from bulky ligands and halogen bridged dinuclear complexes with $Cu_2(\mu\text{-}X)_2$ cores.[56]

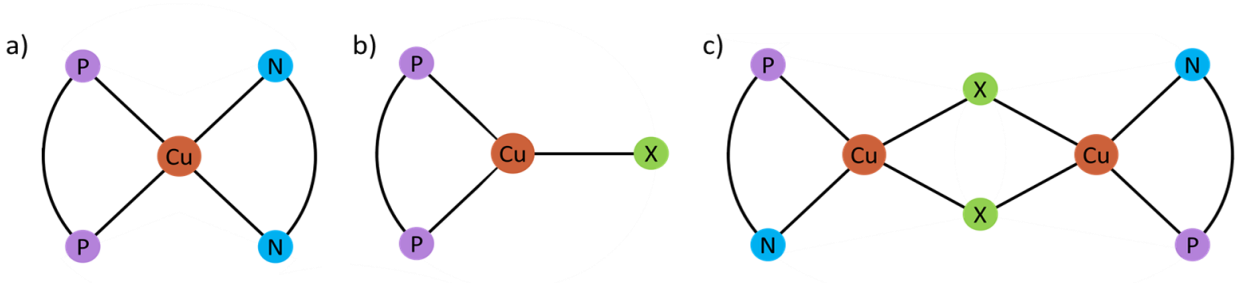

Figure 2.4: General structures for common Copper(I) TADF emitters. a) tetrahedral complexes with donor and acceptor ligand pair, b) triganol planar complexes, and c) dihalide bridged dinuclear complexes

A common ligand pair for tetrahedral complexes comprises bisphosphines and diimines ($Cu(P\hat{}P)(N\hat{}N)]^{+}$).[75,76] Typically for these complexes, the HOMO resides on P-Cu-P and the LUMO in the π^*-orbitals of (N^N) or (P^P), depending on diamine. During excitation, the Cu(I) center is formally oxidized to C(II) (d^9) during MLCT which causes distortion towards a flattened square planar geometry due to a pseudo-Jahn-Teller effect.[77] This results in more non-radiative decay pathways. Thus, bulky ligands and rigid frameworks are used to overcome this and minimize additional non-radiative pathways. Using ligands such diphenyl-bis(pyrazol-1-yl)borate eliminates the need for a counter-ion and makes the complex more stable to sublimation for device fabrication.[78]

POLYMER OLEDS

The semiconducting properties of polyacetylene were first reported in 1977,[79] and resulted in the 2000 Nobel prize in chemistry being awarded to Alan Heeger, Alan Macdiarmid, and Hideki Shirakawa for the discovery and development of conductive polymers.[80] Since then, a huge array of emissive polymers have been reported for electroluminescent devices.[81] Because polymer OLEDs (POLEDs) are made from highly conjugated repeat units, they are able to conduct electricity. Thus, they do not require the multiple transport layers necessary for small molecule OLEDs and can be made as single layer devices (Fig. 2.5).[82] Typical LEDs and small molecule OLEDs use expensive sublimation processes that require thermally stable molecules. On the other hand, Polymer OLEDs can be solution

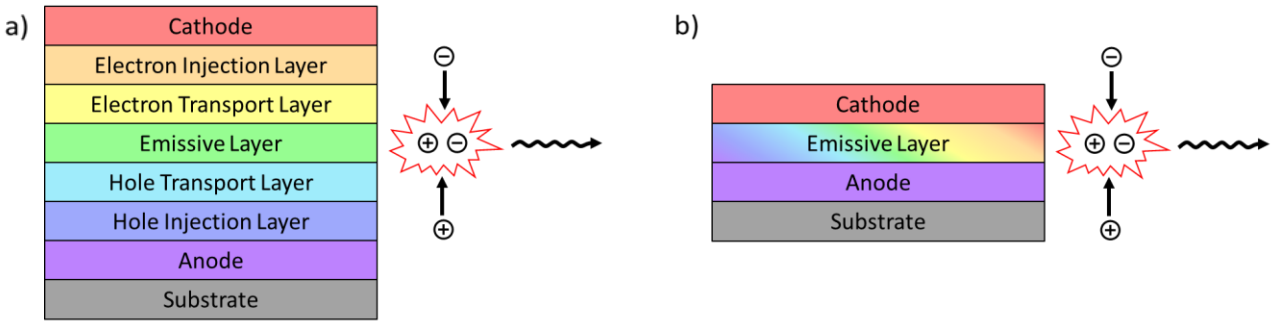

Figure 2.5: Typical constructions for a) a standard small molecule OLED and b) a conductive polymeric OLED

processed and deposited by spin coating or ink-jet printing.[83,84] This also makes polymeric materials more desirable for large area devices.

Discussion

Previous Work

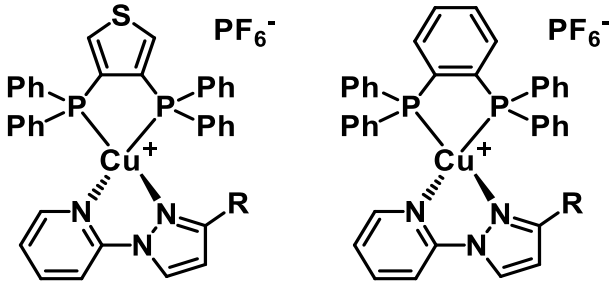

R = CF_3, H, CH_3

Figure 2.6: Cu(I) TADF complexes developed and studied by Dr. Mueller

Dr. Kory Mueller has synthesized a series of Cu(I) TADF complexes with a thiophene bridged bisphosphine (dppt) (Fig. 2.6). This presents a new backbone for these complexes with unique properties compared to more common bridging groups. The corresponding benzene bridged complexes (dppbz) were also synthesized as a direct comparison to these more typical Cu(I) TADF complexes.[85] Studies included

crystallographic data, DFT calculations, electrochemical properties, and extensive investigation of the photophysical properties. The two series of complexes had very similar frontier molecular orbitals and thus similar absorption and emission spectra. The quantum yields of the crystalline powders were near 60 % for all complexes. The wider bite angle from dppt stabilized the HOMO and led to a slight blue shift in the emission spectra relative to the dppbz complexes.[86] The dppt complexes had a decreased lifetime for phosphorescence at 77 K due to increased spin-orbit coupling from the sulfur atom. The thiophene backbone also presents a scaffold for more synthetic flexibility with less expensive starting materials. The two series also showed similar oxidation potentials in their CVs. Unfortunately no electropolymerization was observed for these thiophene complexes.

THIS WORK

To promote electropolymerization, the thiophene backbone could be replaced by the terthiophene analog, 3,4-bis(diphenylphosphino)**ter**thiophene (dppt**, 28**) (Scheme 2.1). This was done by performing a Negishi coupling between tetrabromothiophene and 2 equivalents of 2-bromothiophene.[87] This was then lithiated and reacted with chlorodiphenylphosphine to give the desired ligand. This bis-phosphine oxidizes quickly in solvent exposed to atmosphere, but can be reduced back down using trichlorosilane. An attempt to electropolymerize the free ligand was unsuccessful. This is attributed to the phosphine oxidation inhibiting further oxidative events that would allow for the polymerization. It could also be that the radical generated upon oxidation is dispersed over a large aromatic region in the diphenyl phosphines and is stabilized from polymerizing. This will hopefully be stabilized once coordinated to the Cu(I) center.

Scheme 2.1: Synthetic Strategy for Electropolymerizable Units

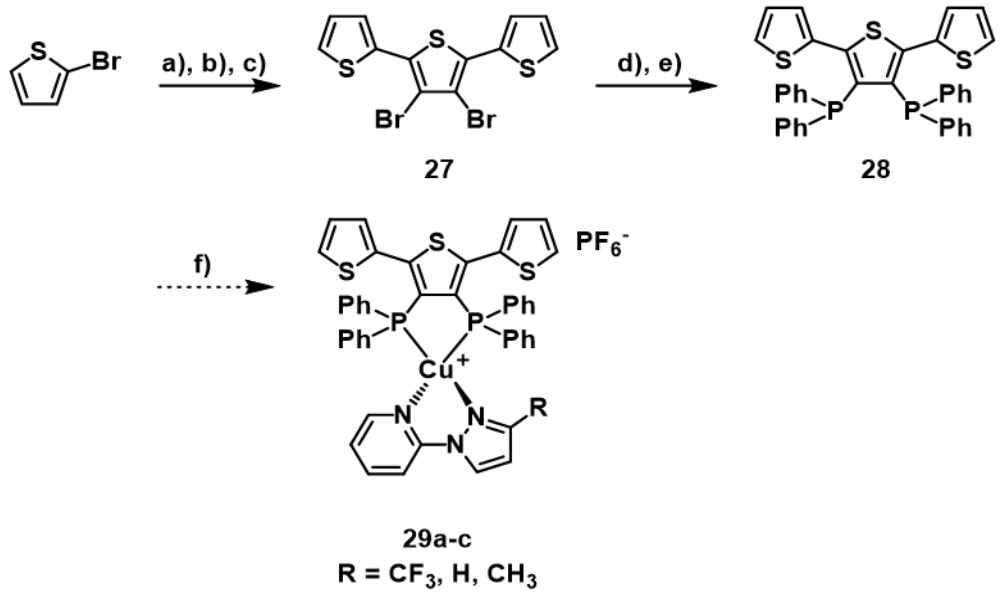

a) *n*-BuLi, Et_2O, -78 °C, 1 h. b) $ZnCl_2$, THF, 0 °C, 1 h. c) 0.02 $Pd(dppf)Cl_2$, tetrabromothiophene, THF, 50 °C, 24 h. d) *n*-BuLi, Et_2O, -78 °C, 45 min. e) $ClPPh_2$, 23 °C, 16h. f) $[Cu(ACN)_4]PF_6$, 2-(pyrazol-1-yl)pyridine, DCM, 23 °C, 2 h.

NEXT STEPS

Continuation of this project would require synthesis and crystallization of the metal complexes. Electropolymerization should proceed more readily than the monothiophene analogs due to lower potential required for oxidation of the polymer and less steric interference. The photophysical and electrochemical properties of both the monomers and polymers should be investigated.

EXPERIMENTAL

Materials and Instrumentation

All chemicals were used as received from vendors. Air and water sensitive reactions were carried out using standard Schlenk techniques under an inert Nitrogen atmosphere. Dry solvents were collected from an Innovative Technology PureSolv 400 solvent purification system and stored over 4 Å molecular sieves. NMR spectra were obtained using an Agilent MR 400 MHz or VARIAN DirectDrive 400 MHz instrument. All chemical shifts are reported in ppm and referenced to residual solvent peaks. Coupling constants are reported in Hertz. Mass spectrometry was carried out on an Agilent 6530 quadrupole time of flight mass spectrometer.

Synthesis

The following compounds were synthesized according to previously reported literature procedures: 2,6-bis(pyrazol-1-yl)pyridine (bppy; **1**)[29]; 2-bromo-6-(pyrazol-1-yl)pyridine[29]; 2,6-bis(4-iodopyrazol-1-yl)pyridine (bppy-I; **2**)[29]; bromotriethylene glycol monomethyl ether (Br-PEG)[31]; 4-iodopyrazole (Pz-I; **13**)[30]; 1-(1-ethoxyethyl)-4-iodopyrazole (**15**)[30]; 1-(tert-butyl) 4-ethyl pyrazole-1,4-dicarboxylate (19)[88]; 1-benzyl-4-iodopyrazole (**25**)[89]; [Cu(2,2'-bipyridine)$_2$]BF_4[90].

1,1-(PYRIDINE-2,6-DIYL)BIS(PYRAZOLE)-4,4-DICARBOXALDEHYDE (3)

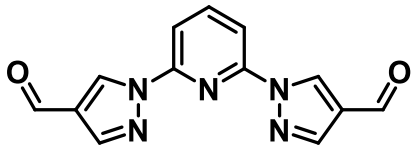

Modified from report by Zoppellaro.[29] In a 250 mL round bottom flask, 2,6-bis(4-iodopyrazol-1-yl)pyridine (0.5060 g, 1.09 mmol) was dissolved in a mixture of THF (25 mL) and diethylether (25 mL). After cooling the solution (-78 °C), *n*-butyllithium (1.6 M in hexanes, 2.05 mL, 4.88 mmol) was added dropwise by syringe. After reacting for 2 hours, DMF (0.4 mL, 5.19 mmol) was added and the solution was left to stir overnight at

room temperature. Water (50 mL) was added to the solution and the organic phase was removed under reduced pressure. The resulting precipitate was collected by vacuum filtration and washed with several small portions of cold acetone (3 x 3 mL). Yield: 0.0873 g, 0.326 mmol, 29.9 %. Characterization previously reported.[91] ^{1}H NMR (400 MHz, DMSO-d_6) δ 9.99 (s, 2H), 9.79 (s, 2H), 8.38 (s, 2H), 8.27 (t, J = 7.9 Hz, 1H), 7.98 (d, J = 8.0 Hz, 2H).

2,6-DI[4-(HYDROXYMETHYL)PYRAZOL-1-YL]PYRIDINE (4)

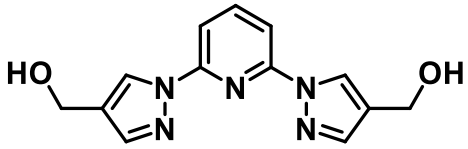

Modified from report by Pritchard.[92] In a 250 mL Schlenk flask, 1,1-(Pyridine-2,6-diyl)bis(pyrazole)-4,4-dicarboxaldehyde (89.5 mg, 0.335 mmol) and $NaBH_4$ (21.4 mg, 0.566 mmol) were dissolved in THF (100 mL). The reaction was refluxed for 3.5 hours and then left to react at room temperature overnight. While stirring, the solution was slowly add to water (50 mL). An HCl solution (0.125 M, 20 mL, 2.5 mmol) was added slowly to the solution to ensure the reaction was fully quenched. The acidic solution was neutralized with aqueous $NaHCO_3$ (1M) until the solution was neutral by litmus paper. The THF in this solution was removed under reduced pressure, and the remaining aqueous phase was extracted with ethyl acetate (3 x 50 mL). The product was purified by column chromatography on silica gel with ethyl acetate eluent. Yield: 16.6 mg, 61.2 µmol, 18.2 %. Characterization previously reported.[92] ^{1}H NMR (400 MHz, Chloroform-d) δ 8.56 (s, 2H), 7.93 (t, J = 7.2 Hz, 1H), 7.82 (d, J = 8.2 Hz, 2H), 7.77 (s, 2H), 4.72 (s, 4H).

2,6-BIS(4-(2,5,8,11-TETRAOXADODECYL)PYRAZOL-1-YL)PYRIDINE (5)

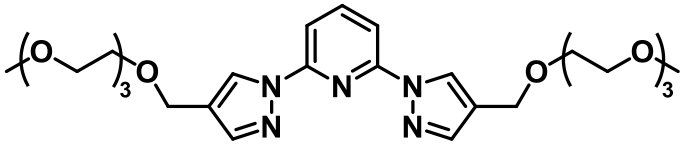

NaH (60 % dispersion in paraffin oil, 0.0442 g, 1.11 mmol) and 2,6-di[4-(hydroxymethyl)pyrazol-1-yl]pyridine (0.017 g, 62.7 µmol) were dissolved in THF (50 mL). After refluxing for 2 hours, bromotriethylene glycol monomethyl ether (0.6787 g, 2.99 mmol) was added via syringe and the reaction continued to reflux overnight. Diethyl ether (30 mL) was added to the solution and then vacuum filtered. The crude filtrate was initially purified by chromatography on silica gel in a 4:1 mixture of hexanes and ethyl acetate solution with 1 % methanol. This eluent mixture was gradually adjusted to ethyl acetate with 1 %. The methanol concentration was then slowly adjusted to 10 % to collect the still crude product. A second column using acetone with 2 % methanol was used to further purify the crude product. Yield: 0.0255 g, 45.3 µmol, 72 %. ^{1}H NMR (400 MHz, Chloroform-*d*) δ 8.56 (s, 2H), 7.92 (dd, *J* = 8.7, 7.2 Hz, 1H), 7.83 (d, *J* = 0.2 Hz, 1H), 7.81 (d, *J* = 1.0 Hz, 1H), 7.75 (s, 2H), 4.57 (s, 4H), 3.70 – 3.67 (m, 14H), 3.66 – 3.63 (m, 6H), 3.56 – 3.52 (m, 4H), 3.36 (s, 6H). HRMS (ESI+): calcd. for $C_{27}H_{41}N_5O_8$ m/z 586.28470 [M+Na]+. Found 586.28470.

2,6-DI[4-(ETHYLCARBOXY)PYRAZOL-1-YL]PYRIDINE (6)

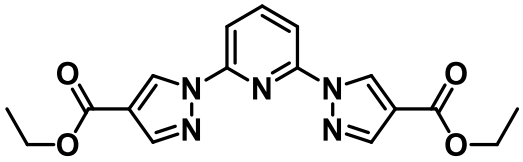

Route A[92]: A solution of NaH (0.3601 g, 9.00 mmol) in diglyme (15 mL) was heated to 70 °C. In an addition funnel, ethyl 1H-pyrazole-4-carboxylate (1.0046 g, 7.17 mmol) in diglyme (15 mL) was added to the solution dropwise. After heating for 1.5 hours, 2,6-dibromopyridine (0.8501 g, 3.59 mmol) was added to the solution. The temperature was increased to 130 °C and the reaction continued for 7 days. After cooling, water (100 mL) was added to the solution. The solution was then extracted with dichloromethane (DCM) (3 x 50 mL), the organic phases were combined, and solvent concentrated under reduced pressure. Water (30 mL) was added to the remaining diglyme and the resulting precipitate was collected by vacuum filtration. The product was purified by chromatography on silica gel with DCM as the eluent. Eluent was adjusted to 5 % MeOH in DCM after remaining

reactants and mono-substituted product had been removed. Yield: 0.4611 g, 1.30 mmol, 36.2 %.

Route B: In a 3-neck round bottom flask equipped with a reflux condenser, 1H-pyrazole-4-carboxylate (0.5053 g, 3.61 mmol) was melted at 100 °C. Slowly, NaH (60 % dispersion in paraffin oil, 0.1480 g, 3.70 mmol) was added while slowly stirring the molten reactant. After 30 minutes, 2,6-dibromopyridine (0.4290 g, 1.80 mmol) was added and the temperature increased to 130 °C and stirred slowly at this temperature for 1 day. After cooling, water (50 mL) and DCM (3 x 50 mL) was used to dissolve and extract the product. The combined organic phases were removed under reduced pressure and the product purified by chromatography on silica gel with DCM as the eluent. Eluent was adjusted to 5 % MeOH in DCM after remaining reactants and mono-substituted product had been removed. Yield: 0.2000 g, 0.563 mmol, 31.3 %.
Characterization previously reported.[92] ^{1}H NMR (400 MHz, Chloroform-*d*) δ 8.95 (s, 2H), 8.06 (s, 2H), 7.93 (t, *J* = 6.6 Hz, 1H), 7.87 (d, *J* = 7.2 Hz, 2H), 4.34 (q, *J* = 7.1 Hz, 4H), 1.38 (t, *J* = 7.1 Hz, 6H). ^{13}C NMR (101 MHz, Chloroform-*d*) δ 162.57, 149.27, 143.17, 141.86, 129.97, 117.34, 110.84, 60.67, 14.39.

ETHYL 1-(6-BROMOPYRIDIN-2-YL)PYRAZOLE-4-CARBOXYLATE (7)

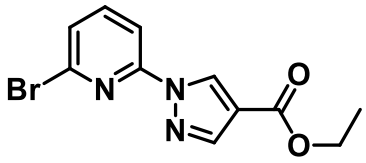

Obtained as the byproduct of the above synthesis. Route A: (0.2139 g, 0.722 mmol, 20.1 % yield). Route B: (0.0303 g, 0.102 mmol, 5.6% yield). Characterization previously reported.[92] ^{1}H NMR (400 MHz, Chloroform-*d*) δ 8.96 (s, 1H), 8.07 (s, 1H), 7.92 (d, *J* = 8.0 Hz, 1H), 7.67 (t, *J* = 7.9 Hz, 1H), 7.41 (d, *J* = 7.7 Hz, 1H), 4.32 (q, *J* = 7.1 Hz, 2H), 1.36 (t, *J* = 7.1 Hz, 3H). ^{13}C NMR (101 MHz, Chloroform-*d*) δ 162.54, 150.54, 143.31, 140.91, 140.09, 130.45, 126.37, 117.28, 111.30, 60.58, 14.35.

ETHYL 1-(6-(PYRAZOL-1-YL)PYRIDIN-2-YL)PYRAZOLE-4-CARBOXYLATE (8)

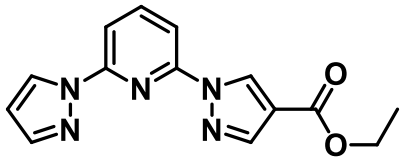

In a nitrogen filled glovebox, ethyl 1H-pyrazole-4-carboxylate (0.5021 g, 3.58 mmol) and NaH (60 % dispersion in paraffin oil, 0.1917 g, 4.79 mmol) were dissolved in diglyme (50 mL). The reaction flask was transferred out of the glovebox and connected to a Schlenk line with a reflux condenser. After the solution was heated to 75 °C for 30 minutes, 2-bromo-6-(pyrazol-1-yl)pyridine (0.7971 g, 3.56 mmol) was added to the solution. The temperature was increased to 115 °C for 3 days. Water (100 mL) and DCM (3 x 50 mL) were added and organic phases were extracted, combined, and solvent concentrated under reduced pressure. Water (30 mL) was added to the remaining diglyme solution and the resulting precipitate was removed by vacuum filtration. The crude product was purified by chromatography on silica with DCM eluent. Yield: 0.4425 g, 1.56 mmol, 43.9 %. ^{1}H NMR (400 MHz, Chloroform-*d*) δ 8.89 (s, 1H), 8.48 (d, *J* = 2.6 Hz, 1H), 8.03 (s, 1H), 7.87 – 7.78 (m, 2H), 7.74 (dd, *J* = 7.2, 1.6 Hz, 1H), 7.69 (s, 1H), 6.43 (dd, *J* = 2.6, 1.7 Hz, 1H), 4.31 (q, *J* = 7.1 Hz, 2H), 1.35 (t, *J* = 7.1 Hz, 3H).

1,1'-(PYRIDINE-2,6-DIYL)BIS(PYRAZOLE-4-CARBOXYLIC ACID) (9)

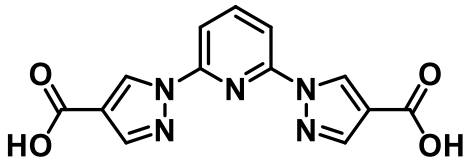

In an open Erlenmeyer flask, NaOH (0.0444 g, 1.11 mmol) was dissolved in a 1:1 mixture of water and ethanol (50 mL each). After adding 2,6-di[4-(ethylcarboxy)pyrazol-1-yl]pyridine (0.1734 g, 0.488 mmol), the solution was heated to boiling until almost all ethanol had been removed. HCl (1 M, 10 mL) was added to the solution and the resulting precipitate was vacuum filtered and washed with water (3 x 15 mL) and small portions of methanol (2 x 3 mL). Yield: 0.1279 g, 0.427 mmol, 87.6 %. ^{1}H NMR (400 MHz, DMSO-

d_6) δ 12.79 (s, 2H), 9.61 (s, 2H), 8.22 (t, *J* = 7.8 Hz, 1H), 8.18 (s, 2H), 7.93 (d, *J* = 8.0 Hz, 2H).

1-(6-(PYRAZOL-1-YL)PYRIDIN-2-YL)PYRAZOLE-4-CARBOXYLIC ACID (10)

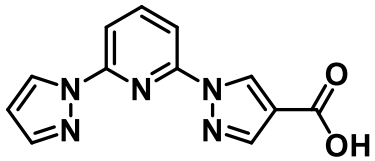

In an open Erlenmeyer flask, NaOH (1.0 M, 1.0 mL, 1.0 mmol) was added to a 1:1 mixture of water and ethanol (50 mL each). After adding 1-(6-(pyrazol-1-yl)pyridin-2-yl)pyrazole-4-carboxylate (0.1102 g, 0.389 mmol), the solution was heated to boiling until almost all ethanol had been removed. HCl (1.0 M, 10 mL) was added to the solution and the resulting precipitate was vacuum filtered and washed with water (3 x 15 mL) and small portions of methanol (2 x 3 mL). Yield: ~ 9.9 mg, 38.9 µmol, 10 %. ^{1}H NMR (400 MHz, DMSO-d_6) δ 12.79 (sb, 1H), 9.39 (s, 1H), 9.10 (dd, *J* = 2.6, 0.7 Hz, 1H), 8.21 – 8.14 (m, 2H), 7.90 – 7.83 (m, 3H), 6.61 (dd, *J* = 2.6, 1.7 Hz, 1H).

2-(4-IODOPYRAZOL-1-YL)-6-(4-(2-(2-(2-METHOXYETHOXY)ETHOXY)ETHYL)PYRAZOL-1-YL)PYRIDINE (11)

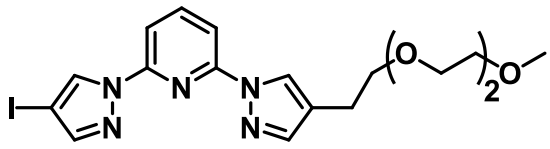

In a Schlenk flask, 2,6-bis(4-iodopyrazol-1-yl)pyridine (0.4964 g, 1.07 mmol) was dissolved in a 1:1 mixture of THF and diethyl ether (25 mL each). After cooling this solution to -78 °C for 30 minutes, *n*-butyllithium (1.6 M, 3.0 mL, 4.8 mmol) was added dropwise by syringe. After stirring at this temperature for 2 hours, 1-bromo-2-(2-(2-methoxyethoxy)ethoxy)ethane (1.1513 g, 5.07 mmol) was added and the reaction was left stirring overnight at room temperature. Water (50 mL) was added slowly to quench the reaction. The organic phase was separate from the aqueous phase and further extracted with DCM (3 x 25 mL). The organic phases were combined and solvent removed under reduced

pressure. The crude product was initially purified by chromatography on silica gel using 4:1 hexanes:ethyl acetate mixture as the eluent. This eluent was gradually adjusted to ethyl acetate with 5 % methanol. The product was further purified on a second column using DCM as the eluent, which was gradually adjusted to DCM with 30 % ethyl acetate. Yield: 0.0468 g, 96.9 µmol, 9.03 %. ^{1}H NMR (400 MHz, Chloroform-*d*) δ 8.56 (d, *J* = 2.7 Hz, 1H), 7.97 – 7.89 (m, 2H), 7.80 (dd, *J* = 7.3, 1.5 Hz, 1H), 7.75 (d, *J* = 1.6 Hz, 1H), 7.65 (s, 1H), 6.50 (dd, *J* = 2.6, 1.7 Hz, 1H), 3.77 (t, *J* = 7.8 Hz, 2H), 3.66 – 3.58 (m, 8H), 3.54 – 3.50 (m, 2H), 3.36 (s, 3H).

1H-PYRAZOLE-4-CARBALDEHYDE (14)

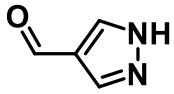

Originally reported by Catala, et al.[32] In a Schlenk flask, 4-iodo-1H-pyrazole (1.0090 g, 5.20 mmol) was dissolved in THF (25 mL). After cooling to -78 °C, *n*-butyllithium (1.6 M in hexanes, 9.8 mL, 15.68 mmol) was added dropwise by syringe. The reaction was stirred cold for 30 minutes and then at room temperature for 3.5 hours. The solution was cooled to -78 °C again, and DMF (0.55 mL, 7.13 mmol) was added dropwise by syringe. After stirring overnight at room temperature, the reaction was quenched with a NH_4Cl solution (1 M, ~25 mL). The solution was then extracted with ether (4 x 60 mL), the organic phases combined, dried over $MgSO_4$, filtered, and solvent removed under reduced pressure. The product was purified by chromatography on silica gel, using DCM with 10% ethyl acetate as the eluent. Yield: 0.0758 g, 0.788 mmol, 15.2 %. Characterization previously reported.[32] ^{1}H NMR (400 MHz, DMSO-d_6) δ 9.82 (s, 1H), 8.00 (s, 2H).

(1H-PYRAZOL-4-YL)METHANOL (18)

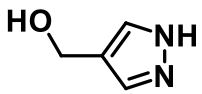

Procedure reported by Bur, et al.[93] In a nitrogen glovebox, ethyl 1H-pyrazole-4-carboxylate (0.9969 g, 7.11 mmol) was dissolved in THF (25 mL), and lithium aluminum hydride

(0.9967 g, 26.23 mmol) was added slowly to this solution. The reaction flask was removed from the glovebox and connected to a Schlenk line and left stirring overnight. The reaction mixture was then neutralized by pouring it into a saturated aqueous solution of Rochelle salt (~25 mL). This mixture was stirred for 3 hours. The solution was extracted with ethyl acetate (5X 25 mL), the organic phases were combined, dried over $MgSO_4$, filtered, and solvent removed under reduced pressure to give the pure product. Yield: 0.3876 g, 3.95 mmol, 55.5 %. Characterization previously reported.[93] ^{1}H NMR (400 MHz, DMSO-d_6) δ 9.82 (s, 1H), 8.00 (s, 2H).

2-(2-(2-(2-METHOXYETHOXY)ETHOXY)ETHOXY)-6-(4-(2-(2-(2-METHOXYETHOXY)ETHOXY)ETHOXY)PYRAZOL-1-YL)PYRIDINE (23)

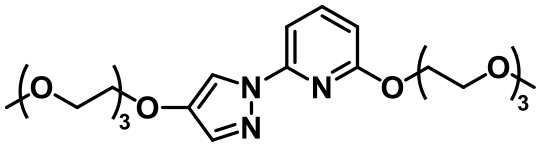

In a round bottom flask equipped with a reflux condenser, 2,6-bis(4-iodopyrazol-1-yl)pyridine (0.3696, 0.857 mmol), monomethoxytriethylene glycol (6 mL, 37.5 mmol), $CsCO_3$ (1.1501 g, 3.55 mmol), CuI (0.0160 g, 84.0 µmol), and 1,10-phenanthroline (0.0153 g, 84.9 µmol) were all combined and refluxed for 20 hours. After cooling, ethyl acetate (25 mL) was added to the solution and then washed with 5 % $NaHCO_3$ in water (4 x 25 mL). The organic phase was dried over Na_2SO_4, filtered, and solvent removed under reduced pressure. The crude product was initially purified by column chromatography on silica gel with 9:1 DCM:acetone, gradually adjusted to just acetone as the eluent. The product was further purified by additional chromatography on silica gel with ethyl acetate as the eluent. Yield: ~0.26 g 0.557 mmol, 65 %. ^{1}H NMR (400 MHz, Chloroform-*d*) δ 8.05 (s, 1H), 7.63 (t, *J* = 7.9 Hz, 1H), 7.47 (s, 1H), 7.41 (d, *J* = 7.8 Hz, 1H), 6.59 (d, *J* = 8.1 Hz, 1H), 4.51 – 4.46 (m, 2H), 4.13 – 4.08 (m, 2H), 3.89 – 3.81 (m, 4H), 3.74 – 3.71 (m, 6H), 3.67 (s, 4H), 3.64 (s, 4H), 3.55 – 3.50 (m, 4H), 3.35 (s, 3H), 3.35 (s, 3H).

2-(4-IODOPYRAZOL-1-YL)-6-(2-(2-(2-METHOXYETHOXY)ETHOXY)ETHOXY)PYRIDINE (24)

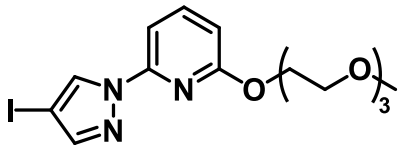

In a Schlenk flask, bppy-I (0.3976 g, 0.858 mmol), K_3PO_4 (0.6466 g, 3.05 mmol), and [Cu(2,2'-bipyridine)$_2$]BF_4 (0.0234 g, 0.0506 mmol), and monomethoxytriethylene glycol (8 mL, 50.0 mmol) were combined and heated near reflux for 1.5 days. After cooling, DCM was added to the solution and filtered. The solvent was removed under reduced pressure and the product purified by column chromatography on silica gel using 2:1 ethyl acetate:hexanes with 2 % methanol as eluent. Yield: 0.2374 g, 0.548 mmol, 63.8 %. ^{1}H NMR (400 MHz, Chloroform-*d*) δ 8.41 (s, 1H), 7.58 (t, *J* = 8.2, 7.7 Hz, 2H), 7.52 (s, 1H), 7.35 (d, *J* = 7.7 Hz, 1H), 6.57 (d, *J* = 8.1 Hz, 1H), 4.43 – 4.38 (m, 2H), 3.81 – 3.76 (m, 2H), 3.67 – 3.62 (m, 2H), 3.62 – 3.53 (m, 4H), 3.48 – 3.42 (m, 2H), 3.27 (s, 3H).

1-BENZYL-4-(2-(2-(2-METHOXYETHOXY)ETHOXY)ETHOXY)PYRAZOLE (26)

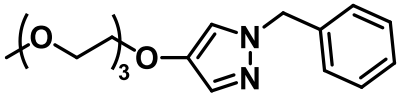

In a Schlenk flask equipped with a reflux condenser, 1-benzyl-4-iodopyrazole (0.5125 g, 1.80 mmol), triethylene glycol monomethyl ether (10 mL, 62.5 mmol), K_3PO_4 (1.0524 g 4.95 mmol), CuI (0.0414 g, 0.217 mmol), and neocuproine (0.0887 g, 0.426 mmol) were all combined and the solution refluxed for 2 days. After cooling, an aqueous $NaHCO_3$ solution (10 %, 40 mL) was added. This solution was extracted with ethyl acetate (50 mL). This organic phase was washed with additional $NaHCO_3$ solution (10 %, 2X 40 mL) and water (3X 30 mL). The product was purified by column chromatography on silica gel with ethyl acetate as the mobile phase. Yield: 0.1621 g, 0.506 mmol, 28.0 %. ^{1}H NMR (400 MHz, Chloroform-*d*) δ 7.29 – 7.23 (m, 3H), 7.22 (d, *J* = 0.8 Hz, 1H), 7.14 – 7.10 (m, 2H), 7.01 (d, *J* = 0.8 Hz, 1H), 5.13 (s, 2H), 3.96 – 3.92 (m, 2H), 3.73 – 3.69 (m, 2H), 3.65 – 3.62 (m, 2H), 3.62 – 3.56 (m, 4H), 3.50 – 3.46 (m, 2H), 3.31 (s, 3H). ^{13}C NMR (101 MHz,

Chloroform-*d*) δ 136.66, 128.70, 127.92, 127.46, 127.34, 114.92, 71.84, 71.05, 70.67, 70.54, 70.46, 69.72, 58.95, 56.54.

3',4'-DIBROMO-2,2':5',2''-TERTHIOPHENE (27)

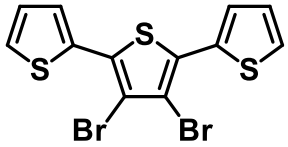

Reported by Mitsudo et al.[87] In a 500 mL Schlenk flask, 2-bromothiphene (4.5 mL, 46 mmol) was dissolved in 45 mL of diethyl ether and cooled to -78 °C before *n*-butyllithium (1.6 M in hexanes, 32 mL, 51 mmol) was added dropwise to the solution via addition funnel. After stirring cold for 1 hour, $ZnCl_2$ (6.3600 g, 46.7 mmol) in THF (90 mL) was added to the solution via cannula. The reaction vessel was then transferred to an ice water bath and stirred for 1 hour. In a separate round bottom flask, tetrabromothiophene (7.4428 g, 18.6 mmol) and $Pd(dppf)Cl_2$ (0.7703 g, 0.941 mmol) was dissolved in THF (40 mL) and then transferred via cannula to the main reaction vessel. The reaction was then heated to 50 °C for 32 hours. The solution was allowed to cool, quenched with saturated NH_4Cl solution (~10 mL), and extracted with ethyl acetate (3 X 50 mL). The organic phases were combined and dried over $MgSO_4$ and concentrated under reduced pressure. The crude product was initially purified via chromatography on silica gel with 2 % THF in hexanes as eluent. The still crude fractions containing the desired product were combined and solvent was removed under reduced pressure. Small portions of hexanes were added to the crude solid, swirled gently, and pipetted off several times until a bright yellow solid remained Yield: 4.0186 g, 9.89 mmol, 53%. Characterization previously reported.[87] ^{1}H NMR (400 MHz, Chloroform-*d*) δ 7.45 (dd, *J* = 3.7, 1.1 Hz, 2H), 7.39 (dd, *J* = 5.1, 1.1 Hz, 2H), 7.09 (dd, *J* = 5.1, 3.7 Hz, 2H). ^{13}C NMR (101 MHz, Chloroform-*d*) δ 133.95, 130.98, 127.36, 127.06, 126.78, 112.33.

3',4'-BIS(DIPHENYLPHOSPHINO)-2,2':5',2''-TERTHIOPHENE (28)

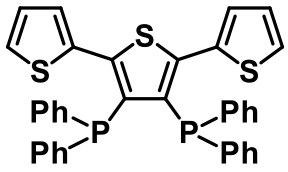

Modified from synthesis reported by Dr. Kory Mueller.[85] Synthesis followed the general procedure reported for the preparation of 3,4-bis(diphenylphosphino)thiophene. All solvents were sparged with nitrogen gas before use in each step of this synthesis. In a 250 mL Schlenk flask, 3',4'-dibromo-2,2':5',2"-terthiophene (0.5040 g, 1.241 mmol) was dissolved in diethyl ether (100 mL) and then cooled to -78 °C for 30 minutes. The solution was stirred as *n*-butyllithium (1.6 M in hexanes, 1.70 mL, 2.72 mmol) was added dropwise via syringe. The solution was left to stir cold for 45 minutes before chlorodiphenylphosphine (0.55 mL, 3.1 mmol) was added dropwise by syringe. The cold bath was removed and the solution allowed to stir at room temperature overnight. Water (70 mL) was added slowly to the reaction mixture and diethyl ether was removed under reduced pressure. The solution was then extracted with DCM (2 x 25 mL). The DCM fractions were combined in a Schlenk flask and concentrated under reduce pressure. Methanol was added to the sealed flask and the solution was allowed to recrystallize in a refrigerator overnight. The resulting yellow crystals were filtered cold and washed with methanol (3 x 10 mL). The filtrate was concentrated and crystalized a second time to improve the overall yield (0.4725 g, 0.7661 mmol, 62% yield). Alternatively, the extracted crude solution can be purified by chromatography on silica gel using 30% DCM in hexanes as eluent. ^{1}H NMR (400 MHz, Methylene Chloride-d_2) δ 7.24 – 7.19 (m, 9H), 7.15 – 7.11 (m, 13H), 7.09 (dd, J = 5.1, 1.3 Hz, 2H), 6.64 (dd, J = 5.1, 3.6 Hz, 2H), 6.60 (dd, J = 3.6, 1.3 Hz, 2H). ^{31}P NMR (162 MHz, Methylene Chloride-d_2) δ -17.79.

REFERENCES

1. Bünzli, J.-C. G., Lanthanide Luminescence for Biomedical Analyses and Imaging. *Chemical Reviews* **2010,** *110* (5), 2729-2755.
2. Shibasaki, M.; Yoshikawa, N., Lanthanide Complexes in Multifunctional Asymmetric Catalysis. *Chemical Reviews* **2002,** *102* (6), 2187-2210.
3. Cockerill, A. F.; Davies, G. L. O.; Harden, R. C.; Rackham, D. M., Lanthanide shift reagents for nuclear magnetic resonance spectroscopy. *Chemical Reviews* **1973,** *73* (6), 553-588.
4. Wang, K.-M.; Du, L.; Ma, Y.-L.; Zhao, J.-S.; Wang, Q.; Yan, T.; Zhao, Q.-H., Multifunctional chemical sensors and luminescent thermometers based on lanthanide metal–organic framework materials. *CrystEngComm* **2016,** *18* (15), 2690-2700.
5. Rocha, J.; Brites, C. D. S.; Carlos, L. D., Lanthanide Organic Framework Luminescent Thermometers. *Chemistry – A European Journal* **2016,** *22* (42), 14782-14795.
6. Woodruff, D. N.; Winpenny, R. E. P.; Layfield, R. A., Lanthanide Single-Molecule Magnets. *Chemical Reviews* **2013,** *113* (7), 5110-5148.
7. Hasegawa, Y.; Kawai, H.; Nakamurea, K.; Yasuda, N.; Wada, Y.; Yanagida, S., Molecular design of luminsecent Eu(III) complexes as lanthanide lasing material and their optical properties. *Journal of Alloys and Compounds* **2006,** *408-412*, 669-674.
8. Yang, C.; Sun, Z.-F.; Liu, L.; Zhang, L.-Q., Preparation and luminescence performance of rare earth agriculture-used light transformation composites. *Journal of Materials Science* **2008,** *43* (5), 1681-1687.
9. Taydakov, I. V.; Akkuzina, A. A.; Avetisov, R. I.; Khomyakov, A. V.; Saifutyarov, R. R.; Avetissov, I. C., Effective electroluminescent materials for OLED applications based on lanthanide 1.3-diketonates bearing pyrazole moiety. *Journal of Luminescence* **2016,** *177*, 31-39.
10. Stanley, J. M.; Holliday, B. J., Luminescent lanthanide-containing metallopolymers. *Coordination Chemistry Reviews* **2012,** *256* (15), 1520-1530.
11. Li, X.-Z.; Zhou, L.-P.; Yan, L.-L.; Dong, Y.-M.; Bai, Z.-L.; Sun, X.-Q.; Diwu, J.; Wang, S.; Bünzli, J.-C.; Sun, Q.-F., A supramolecular lanthanide separation approach based on multivalent cooperative enhancement of metal ion selectivity. *Nature Communications* **2018,** *9* (1), 547.
12. Ward, M. D., Mechanisms of sensitization of lanthanide(III)-based luminescence in transition metal/lanthanide and anthracene/lanthanide dyads. *Coordination Chemistry Reviews* **2010,** *254* (21), 2634-2642.
13. Armelao, L.; Quici, S.; Barigelletti, F.; Accorsi, G.; Bottaro, G.; Cavazzini, M.; Tondello, E., Design of luminescent lanthanide complexes: From molecules to highly efficient photo-emitting materials. *Coordination Chemistry Reviews* **2010,** *254* (5), 487-505.
14. Bünzli, J.-C. G.; Piguet, C., Taking advantage of luminescent lanthanide ions. *Chemical Society Reviews* **2005,** *34* (12), 1048-1077.

15. Rudzinski, C. M.; Engebretson, D. S.; Hartmann, W. K.; Nocera, D. G., Mechanism for the Sensitized Luminescence of a Lanthanide Ion Macrocycle Appended to a Cyclodextrin. *The Journal of Physical Chemistry A* **1998,** *102* (38), 7442-7446.
16. dos Santos, C. M. G.; Harte, A. J.; Quinn, S. J.; Gunnlaugsson, T., Recent developments in the field of supramolecular lanthanide luminescent sensors and self-assemblies. *Coordination Chemistry Reviews* **2008,** *252* (23), 2512-2527.
17. Latva, M.; Takalo, H.; Mukkala, V.-M.; Matachescu, C.; Rodríguez-Ubis, J. C.; Kankare, J., Correlation between the lowest triplet state energy level of the ligand and lanthanide(III) luminescence quantum yield. *Journal of Luminescence* **1997,** *75* (2), 149-169.
18. Meshkova, S. B.; Topilova, Z. M.; Lozinskii, M. O.; Bol'shoi, D. V., Luminescence quenching of lanthanides in complexes with β-diketones containing different fluorinated radicals. *Journal of Applied Spectroscopy* **1997,** *64* (2), 229-233.
19. Ward, M. D., Transition-metal sensitised near-infrared luminescence from lanthanides in d–f heteronuclear arrays. *Coordination Chemistry Reviews* **2007,** *251* (13), 1663-1677.
20. Horrocks, W. D.; Bolender, J. P.; Smith, W. D.; Supkowski, R. M., Photosensitized Near Infrared Luminescence of Ytterbium(III) in Proteins and Complexes Occurs via an Internal Redox Process. *Journal of the American Chemical Society* **1997,** *119* (25), 5972-5973.
21. Hebbink, G. A.; Klink, S. I.; Grave, L.; Oude Alink, P. G. B.; van Veggel, F. C. J. M., Singlet Energy Transfer as the Main Pathway in the Sensitization of Near-Infrared Nd3+ Luminescence by Dansyl and Lissamine Dyes. *ChemPhysChem* **2002,** *3* (12), 1014-1018.
22. Heffern, M. C.; Matosziuk, L. M.; Meade, T. J., Lanthanide Probes for Bioresponsive Imaging. *Chemical Reviews* **2014,** *114* (8), 4496-4539.
23. Wilkerson, J. Luminescent Lanthanide-Containing Materials: From Small Molecules to Conducting Metallopolymers. PhD. Dissertation, University of Texas at Austin, Austin, TX, 2012.
24. Brunet, E.; Juanes, O.; Sedano, R.; Rodríguez-Ubis, J.-C., Lanthanide complexes of polycarboxylate-bearing dipyrazolylpyridine ligands with near-unity luminescence quantum yields: the effect of pyridine substitution. *Photochemical & Photobiological Sciences* **2002,** *1* (8), 613-618.
25. Strohecker, D. J.; Lynch, V. M.; Holliday, B. J.; Jones, R. A., Synthesis and electronic investigation of mono- and di-substituted 4-nitro- and 4-amino-pyrazol-1-yl bis(pyrazol-1-yl)pyridine-type ligands and luminescent Eu(iii) derivatives. *Dalton Transactions* **2017,** *46* (24), 7733-7742.
26. Stanley, J. M.; Zhu, X.; Yang, X.; Holliday, B. J., Europium Complexes of a Novel Ethylenedioxythiophene-Derivatized Bis(pyrazolyl)pyridine Ligand Exhibiting Efficient Lanthanide Sensitization. *Inorganic Chemistry* **2010,** *49* (5), 2035-2037.
27. Narayana, Y. S. L. V.; Baumgarten, M.; Müllen, K.; Chandrasekar, R., Tuning the Solid State Emission of Thin Films/Microspheres Obtained from Alternating Oligo(3-

octylthiophenes) and 2,6-Bis(pyrazole)pyridine Copolymers by Varying Conjugation Length and Eu3+/Tb3+ Metal Coordination. *Macromolecules* **2015,** *48* (14), 4801-4812.
28. Liang, Y. New Materials for Advanced Applications: Electrochromism, Electrocatalysis, and Bioimaging. PhD. Dissertation, University of Texas at Austin, Austin, TX, 2017.
29. Zoppellaro, G.; Baumgarten, M., One-Step Synthesis of Symmetrically Substituted 2,6-Bis(pyrazol-1-yl)pyridine Systems. *European Journal of Organic Chemistry* **2005,** *2005* (14), 2888-2892.
30. Vasilesvsky, S. F.; Klyatskaya, S. V.; Tretyakov, E. V.; Elguero, J., Ethyl vinyl Ether - An Agent for Protection of the Pyrazole NH-fragment. A Convenient Method for the Preparation of N-Unsubstituted 4-Alkynylpyrazoles. *Heterocycles* **2003,** *60* (4), 879-886.
31. Karimi, B.; Mansouri, F.; Vali, H., A highly water-dispersible/magnetically separable palladium catalyst based on a Fe3O4@SiO2 anchored TEG-imidazolium ionic liquid for the Suzuki–Miyaura coupling reaction in water. *Green Chemistry* **2014,** *16* (5), 2587-2596.
32. Catala, L.; Wurst, K.; Amabilino, D. B.; Veciana, J., Polymorphs of a pyrazole nitronyl nitroxide and its complexes with metal(ii) hexafluoroacetylacetonates. *Journal of Materials Chemistry* **2006,** *16* (26), 2736-2745.
33. Taydakov, I. V.; Krasnoselskiy, S. S.; Dutova, T. Y., Improved Synthesis of 1H-Pyrazole-4-carbaldehyde. *Synthetic Communications* **2011,** *41* (16), 2430-2434.
34. Zoppellaro, G.; Enkelmann, V.; Geies, A.; Baumgarten, M., A Multifunctional High-Spin Biradical Pyrazolylbipyridine-bisnitronylnitroxide. *Organic Letters* **2004,** *6* (26), 4929-4932.
35. Nystrom, R. F.; Brown, W. G., Reduction of Organic Compounds by Lithium Aluminum Hydride. I. Aldehydes, Ketones, Esters, Acid Chlorides and Acid Anhydrides. *Journal of the American Chemical Society* **1947,** *69* (5), 1197-1199.
36. Borkin, D.; Pollock, J.; Kempinska, K.; Purohit, T.; Li, X.; Wen, B.; Zhao, T.; Miao, H.; Shukla, S.; He, M.; Sun, D.; Cierpicki, T.; Grembecka, J., Property Focused Structure-Based Optimization of Small Molecule Inhibitors of the Protein–Protein Interaction between Menin and Mixed Lineage Leukemia (MLL). *Journal of Medicinal Chemistry* **2016,** *59* (3), 892-913.
37. Fanta, P. E., The Ullmann Synthesis of Biaryls. *Synthesis* **1974,** *1974* (01), 9-21.
38. Sambiagio, C.; Marsden, S. P.; Blacker, A. J.; McGowan, P. C., Copper catalysed Ullmann type chemistry: from mechanistic aspects to modern development. *Chemical Society Reviews* **2014,** *43* (10), 3525-3550.
39. Chen, H.-W.; Lee, J.-H.; Lin, B.-Y.; Chen, S.; Wu, S.-T., Liquid crystal display and organic light-emitting diode display: present status and future perspectives. *Light: Science &Amp; Applications* **2018,** *7*, 17168.
40. Woon Park, J., 19 - Large-area OLED lighting panels and their applications. In *Organic Light-Emitting Diodes (OLEDs)*, Buckley, A., Ed. Woodhead Publishing: 2013; pp 572-600.

41. Meyer, J.; Görrn, P.; Riedl, T., 17 - Transparent OLED displays. In *Organic Light-Emitting Diodes (OLEDs)*, Buckley, A., Ed. Woodhead Publishing: 2013; pp 512-547.
42. Adachi, C., *Third-generation organic electroluminescence materials†*. 2014; Vol. 53, p 060101.
43. Pardo, D. A.; Jabbour, G. E.; Peyghambarian, N., Application of Screen Printing in the Fabrication of Organic Light-Emitting Devices. *Advanced Materials* **2000,** *12* (17), 1249-1252.
44. Tao, Y.; Yuan, K.; Chen, T.; Xu, P.; Li, H.; Chen, R.; Zheng, C.; Zhang, L.; Huang, W., Thermally Activated Delayed Fluorescence Materials Towards the Breakthrough of Organoelectronics. *Advanced Materials* **2014,** *26* (47), 7931-7958.
45. Zhao, J.; Ji, S.; Guo, H., Triplet–triplet annihilation based upconversion: from triplet sensitizers and triplet acceptors to upconversion quantum yields. *RSC Advances* **2011,** *1* (6), 937-950.
46. Manna, M. K.; Shokri, S.; Wiederrecht, G. P.; Gosztola, D. J.; Ayitou, A. J.-L., New perspectives for triplet–triplet annihilation based photon upconversion using all-organic energy donor & acceptor chromophores. *Chemical Communications* **2018,** *54* (46), 5809-5818.
47. Xu, H.; Chen, R.; Sun, Q.; Lai, W.; Su, Q.; Huang, W.; Liu, X., Recent progress in metal–organic complexes for optoelectronic applications. *Chemical Society Reviews* **2014,** *43* (10), 3259-3302.
48. Minaev, B.; Baryshnikov, G.; Agren, H., Principles of phosphorescent organic light emitting devices. *Physical Chemistry Chemical Physics* **2014,** *16* (5), 1719-1758.
49. S. Mehta, D.; Saxena, K., *Light out-coupling strategies in organic light emitting devices*. 2019.
50. Wang, Z. B.; Helander, M. G.; Qiu, J.; Puzzo, D. P.; Greiner, M. T.; Hudson, Z. M.; Wang, S.; Liu, Z. W.; Lu, Z. H., Unlocking the full potential of organic light-emitting diodes on flexible plastic. *Nature Photonics* **2011,** *5*, 753.
51. Shakeel, U.; Singh, J., Study of processes of reverse intersystem crossing (RISC) and thermally activated delayed fluorescence (TADF) in organic light emitting diodes (OLEDs). *Organic Electronics* **2018,** *59*, 121-124.
52. Lee, S. Y.; Yasuda, T.; Nomura, H.; Adachi, C., High-efficiency organic light-emitting diodes utilizing thermally activated delayed fluorescence from triazine-based donor–acceptor hybrid molecules. *Applied Physics Letters* **2012,** *101* (9), 093306.
53. Hosokai, T.; Matsuzaki, H.; Nakanotani, H.; Tokumaru, K.; Tsutsui, T.; Furube, A.; Nasu, K.; Nomura, H.; Yahiro, M.; Adachi, C., Evidence and mechanism of efficient thermally activated delayed fluorescence promoted by delocalized excited states. *Science Advances* **2017,** *3* (5), e1603282.
54. Im, Y.; Kim, M.; Cho, Y. J.; Seo, J.-A.; Yook, K. S.; Lee, J. Y., Molecular Design Strategy of Organic Thermally Activated Delayed Fluorescence Emitters. *Chemistry of Materials* **2017,** *29* (5), 1946-1963.
55. Nakagawa, T.; Ku, S.-Y.; Wong, K.-T.; Adachi, C., Electroluminescence based on thermally activated delayed fluorescence generated by a spirobifluorene donor–acceptor structure. *Chemical Communications* **2012,** *48* (77), 9580-9582.

56. Nozaki, K.; Iwamura, M., Highly Emissive d 10 Metal Complexes as TADF Emitters with Versatile Structures and Photophysical Properties. In *Highly Efficient OLEDs: Materials Based on Thermally Activated Delayed Fluorescence*, Yersin, H., Ed. 2018; pp 61-91.
57. Berberan-Santos, M. N.; Garcia, J. M. M., Unusually Strong Delayed Fluorescence of C70. *Journal of the American Chemical Society* **1996,** *118* (39), 9391-9394.
58. Zalibera, M.; Krylov, D. S.; Karagiannis, D.; Will, P.-A.; Ziegs, F.; Schiemenz, S.; Lubitz, W.; Reineke, S.; Savitsky, A.; Popov, A. A., Thermally Activated Delayed Fluorescence in a Y3N@C80 Endohedral Fullerene: Time-Resolved Luminescence and EPR Studies. *Angewandte Chemie International Edition* **2018,** *57* (1), 277-281.
59. Salazar, F. A.; Fedorov, A.; Berberan-Santos, M. N., A study of thermally activated delayed fluorescence in C60. *Chemical Physics Letters* **1997,** *271* (4), 361-366.
60. Hatakeyama, T.; Shiren, K.; Nakajima, K.; Nomura, S.; Nakatsuka, S.; Kinoshita, K.; Ni, J.; Ono, Y.; Ikuta, T., Ultrapure Blue Thermally Activated Delayed Fluorescence Molecules: Efficient HOMO–LUMO Separation by the Multiple Resonance Effect. *Advanced Materials* **2016,** *28* (14), 2777-2781.
61. Gildea, L. F.; Williams, J. A. G., 3 - Iridium and platinum complexes for OLEDs. In *Organic Light-Emitting Diodes (OLEDs)*, Buckley, A., Ed. Woodhead Publishing: 2013; pp 77-113.
62. Choy, W. C. H.; Chan, W. K.; Yuan, Y., Recent Advances in Transition Metal Complexes and Light-Management Engineering in Organic Optoelectronic Devices. *Advanced Materials* **2014,** *26* (31), 5368-5399.
63. Yersin, H.; Rausch, A. F.; Czerwieniec, R.; Hofbeck, T.; Fischer, T., The triplet state of organo-transition metal compounds. Triplet harvesting and singlet harvesting for efficient OLEDs. *Coordination Chemistry Reviews* **2011,** *255* (21), 2622-2652.
64. Uoyama, H.; Goushi, K.; Shizu, K.; Nomura, H.; Adachi, C., Highly efficient organic light-emitting diodes from delayed fluorescence. *Nature* **2012,** *492*, 234.
65. Wong, M. Y.; Zysman-Colman, E., Purely Organic Thermally Activated Delayed Fluorescence Materials for Organic Light-Emitting Diodes. *Advanced Materials* **2017,** *29* (22), 1605444.
66. Okano, Y.; Ohara, H.; Kobayashi, A.; Yoshida, M.; Kato, M., Systematic Introduction of Aromatic Rings to Diphosphine Ligands for Emission Color Tuning of Dinuclear Copper(I) Iodide Complexes. *Inorganic Chemistry* **2016,** *55* (11), 5227-5236.
67. Kim, S.; Bae, H. J.; Park, S.; Kim, W.; Kim, J.; Kim, J. S.; Jung, Y.; Sul, S.; Ihn, S.-G.; Noh, C.; Kim, S.; You, Y., Degradation of blue-phosphorescent organic light-emitting devices involves exciton-induced generation of polaron pair within emitting layers. *Nature Communications* **2018,** *9* (1), 1211.
68. Zhang, Q.; Li, B.; Huang, S.; Nomura, H.; Tanaka, H.; Adachi, C., Efficient blue organic light-emitting diodes employing thermally activated delayed fluorescence. *Nature Photonics* **2014,** *8*, 326.
69. Kochmann, S.; Baleizão, C.; Berberan-Santos, M. N.; Wolfbeis, O. S., Sensing and Imaging of Oxygen with Parts per Billion Limits of Detection and Based on the Quenching

of the Delayed Fluorescence of 13C70 Fullerene in Polymer Hosts. *Analytical Chemistry* **2013,** *85* (3), 1300-1304.
70. Baleizão, C.; Nagl, S.; Schäferling, M.; Berberan-Santos, M. N.; Wolfbeis, O. S., Dual Fluorescence Sensor for Trace Oxygen and Temperature with Unmatched Range and Sensitivity. *Analytical Chemistry* **2008,** *80* (16), 6449-6457.
71. Liu, J.; Wang, N.; Yu, Y.; Yan, Y.; Zhang, H.; Li, J.; Yu, J., Carbon dots in zeolites: A new class of thermally activated delayed fluorescence materials with ultralong lifetimes. *Science Advances* **2017,** *3* (5), e1603171.
72. Xiong, X.; Song, F.; Wang, J.; Zhang, Y.; Xue, Y.; Sun, L.; Jiang, N.; Gao, P.; Tian, L.; Peng, X., Thermally Activated Delayed Fluorescence of Fluorescein Derivative for Time-Resolved and Confocal Fluorescence Imaging. *Journal of the American Chemical Society* **2014,** *136* (27), 9590-9597.
73. Yu, Z.-J.; Lou, W.-Y.; Junge, H.; Päpcke, A.; Chen, H.; Xia, L.-M.; Xu, B.; Wang, M.-M.; Wang, X.-J.; Wu, Q.-A.; Lou, B.-Y.; Lochbrunner, S.; Beller, M.; Luo, S.-P., Thermally activated delayed fluorescence (TADF) dyes as efficient organic photosensitizers for photocatalytic water reduction. *Catalysis Communications* **2019,** *119*, 11-15.
74. Osawa, M.; Hoshino, M., Molecular Design and Synthesis of Metal Complexes as Emitters for TADF-Type OLEDs. In *Highly Efficient OLEDs: Materials Based on Thermally Activated Delayed Fluorescence*, Yersin, H., Ed. 2018; pp 119-176.
75. Czerwieniec, R.; Yersin, H., Diversity of Copper(I) Complexes Showing Thermally Activated Delayed Fluorescence: Basic Photophysical Analysis. *Inorganic Chemistry* **2015,** *54* (9), 4322-4327.
76. Chen, X.-L.; Yu, R.; Zhang, Q.-K.; Zhou, L.-J.; Wu, X.-Y.; Zhang, Q.; Lu, C.-Z., Rational Design of Strongly Blue-Emitting Cuprous Complexes with Thermally Activated Delayed Fluorescence and Application in Solution-Processed OLEDs. *Chemistry of Materials* **2013,** *25* (19), 3910-3920.
77. Czerwieniec, R.; Leitl, M. J.; Homeier, H. H. H.; Yersin, H., Cu(I) complexes – Thermally activated delayed fluorescence. Photophysical approach and material design. *Coordination Chemistry Reviews* **2016,** *325*, 2-28.
78. Igawa, S.; Hashimoto, M.; Kawata, I.; Yashima, M.; Hoshino, M.; Osawa, M., Highly efficient green organic light-emitting diodes containing luminescent tetrahedral copper(i) complexes. *Journal of Materials Chemistry C* **2013,** *1* (3), 542-551.
79. Chiang, C. K.; Fincher, C. R.; Park, Y. W.; Heeger, A. J.; Shirakawa, H.; Louis, E. J.; Gau, S. C.; MacDiarmid, A. G., Electrical Conductivity in Doped Polyacetylene. *Physical Review Letters* **1977,** *39* (17), 1098-1101.
80. The Nobel Prize in Chemistry 2000. https://www.nobelprize.org/prizes/chemistry/2000/summary/ (accessed Mar 26, 2019).
81. Grimsdale, A. C.; Leok Chan, K.; Martin, R. E.; Jokisz, P. G.; Holmes, A. B., Synthesis of Light-Emitting Conjugated Polymers for Applications in Electroluminescent Devices. *Chemical Reviews* **2009,** *109* (3), 897-1091.
82. Kabra, D.; Lu, L. P.; Song, M. H.; Snaith, H. J.; Friend, R. H., Efficient Single-Layer Polymer Light-Emitting Diodes. *Advanced Materials* **2010,** *22* (29), 3194-3198.

83. Sekine, C.; Tsubata, Y.; Yamada, T.; Kitano, M.; Doi, S., Recent progress of high performance polymer OLED and OPV materials for organic printed electronics. *Science and Technology of Advanced Materials* **2014,** *15* (3), 034203.
84. Nuyken, O.; Jungermann, S.; Wiederhirn, V.; Bacher, E.; Meerholz, K., Modern Trends in Organic Light-Emitting Devices (OLEDs). *Monatshefte für Chemie / Chemical Monthly* **2006,** *137* (7), 811-824.
85. Mueller, K. New Approaches to Functional Organic Electronics: Developoment of Redox Active Materials for Energy Applications. PhD. Dissertation, University of Texas at Austin, Austin, TX, 2016.
86. Saito, K.; Arai, T.; Takahashi, N.; Tsukuda, T.; Tsubomura, T., A series of luminescent Cu(i) mixed-ligand complexes containing 2,9-dimethyl-1,10-phenanthroline and simple diphosphine ligands. *Dalton Transactions* **2006,** (37), 4444-4448.
87. Mitsudo, K.; Sato, H.; Yamasaki, A.; Kamimoto, N.; Goto, J.; Mandai, H.; Suga, S., Synthesis and Properties of Ethene-Bridged Terthiophenes. *Organic Letters* **2015,** *17* (19), 4858-4861.
88. Naud, S.; Westwood, I. M.; Faisal, A.; Sheldrake, P.; Bavetsias, V.; Atrash, B.; Cheung, K.-M. J.; Liu, M.; Hayes, A.; Schmitt, J.; Wood, A.; Choi, V.; Boxall, K.; Mak, G.; Gurden, M.; Valenti, M.; de Haven Brandon, A.; Henley, A.; Baker, R.; McAndrew, C.; Matijssen, B.; Burke, R.; Hoelder, S.; Eccles, S. A.; Raynaud, F. I.; Linardopoulos, S.; van Montfort, R. L. M.; Blagg, J., Structure-Based Design of Orally Bioavailable 1H-Pyrrolo[3,2-c]pyridine Inhibitors of Mitotic Kinase Monopolar Spindle 1 (MPS1). *Journal of Medicinal Chemistry* **2013,** *56* (24), 10045-10065.
89. Kahraman, M.; Borchardt, A. J.; Davis, R. L.; Noble, S. A.; Malecha, J. W. Carbazole Inhibitors of Histamine Receptors for the Treatment of Disease. US 8,080,566 B1, Dec 20, 2011.
90. Niu, J.; Zhou, H.; Li, Z.; Xu, J.; Hu, S., An Efficient Ullmann-Type C−O Bond Formation Catalyzed by an Air-Stable Copper(I)−Bipyridyl Complex. *The Journal of Organic Chemistry* **2008,** *73* (19), 7814-7817.
91. Zoppellaro, G.; Geies, A.; Enkelmann, V.; Baumgarten, M., 2,6-Bis(pyrazolyl)pyridine Functionalised with Two Nitronylnitroxide and Iminonitroxide Radicals. *European Journal of Organic Chemistry* **2004,** *2004* (11), 2367-2374.
92. Pritchard, R.; Kilner, C. A.; Barrett, S. A.; Halcrow, M. A., Two new 4′,4″-disubstituted dipyrazolylpyridine derivatives, and the structures and spin states of their iron(II) complexes. *Inorganica Chimica Acta* **2009,** *362* (12), 4365-4371.
93. Bur, D.; Gude, M.; Hubschwerlen, C.; Panchaud, P. Isoquinolin-3-ylurea Derivatives. US 2013/0096119 A1, Apr 18, 2013.